Transcriptional organization and regulation of the *Pseudomonas putida* flagellar system

Antonio Leal-Morales¶, Marta Pulido-Sánchez¶, Aroa López-Sánchez and Fernando Govantes*

Running title: Regulation of *P. putida* flagellar genes

Centro Andaluz de Biología del Desarrollo, Universidad Pablo de Olavide/Consejo Superior de Investigaciones Científicas/Junta de Andalucía and Departamento de Biología Molecular e Ingeniería Bioquímica, Universidad Pablo de Olavide, Sevilla, Spain.

*Corresponding author. Address: Centro Andaluz de Biología del Desarrollo, Universidad Pablo de Olavide, Carretera de Utrera, Km. 1, 41013, Sevilla, Spain. Phone: +34 954349386. Fax: +34 954349376. E-mail: fgovrom@upo.es

¶These authors contributed equally to the work presented

22 **ORIGINALITY-SIGNIFICANCE STATEMENT**

23 This is the first integrative study of the flagellar transcriptional cascade in
24 *Pseudomonas putida*. Our results provide a new transcriptional organization featuring
25 several operons with a nested architecture, detailed regulatory characterization of twenty-
26 two flagellar promoters and a novel hierarchy for the regulatory circuit of the flagellar
27 transcriptional cascade. The results presented represent a significant departure from
28 previous models for other related bacteria. High conservation of flagellar gene organization
29 and promoter sequences suggest that our observations may be relevant to other
30 pseudomonads.

31

SUMMARY

A single region of the *Pseudomonas putida* genome, designated the flagellar cluster, includes 59 genes potentially involved in the biogenesis and function of the flagellar system. Here we combine bioinformatics and *in vivo* gene expression analyses to clarify the transcriptional organization and regulation of the flagellar genes in the cluster. We have identified eleven flagellar operons and characterized twenty-two primary and internal promoter regions. Our results indicate that synthesis of the flagellar apparatus and core chemotaxis machinery is regulated by a three-tier cascade in which *fleQ* is a Class I gene, standing at the top of the transcriptional hierarchy. FleQ- and σ^{54}-dependent Class II genes encode most components of the flagellar structure, part of the chemotaxis machinery and multiple regulatory elements, including the flagellar σ factor FliA. FliA activation of Class III genes enables synthesis of the filament, one stator complex and completion of the chemotaxis apparatus. Accessory regulatory proteins and an intricate operon architecture add complexity to the regulation by providing feedback and feed-forward loops to the main circuit. Because of the high conservation of the gene arrangement and promoter motifs, we believe that the regulatory circuit presented here may also apply to other environmental pseudomonads.

50 **INTRODUCTION**

51 Motility allows bacterial cells to colonize new niches and escape from unfavourable
52 habitats, minimizing the negative effects of competition and depletion of local resources
53 (McDougald *et al*., 2012). For many bacteria, motility is directed by flagella, complex
54 molecular machines that enable swimming of individual cells in liquid and semi-solid media
55 and collective swarming on humid surfaces by engaging in propeller-like rotation driven by
56 the proton-motive force (Altegoer *et al*., 2014; Kearns, 2010). The flagella-associated
57 chemotaxis machinery, comprised of membrane-bound chemoreceptors and associated
58 signal transduction proteins, promotes directional motion by controlling flagellar rotation in
59 response to chemical gradients of attractants and repellents (Sourjik and Wingreen, 2012).

60 Bacterial flagella are proteinaceous appendages composed of over 30 different
61 polypeptides (Altegoer *et al*., 2014). Flagella are constituted of three functional units: the
62 basal body, a rotary machine embedded in the cell envelope; the filament, a long and thin
63 helical appendage that protrudes from the cells and acts as a propeller; and the hook, a
64 rigid, curved element that connects basal body and filament. The basal body is the most
65 complex of these units. In Gram-negative bacteria, it is comprised of five separate
66 components: (i) the MS-ring, an annular structure bound to the cell membrane, provides
67 support to the complete flagellar architecture; (ii) attached to the MS-ring, the cytoplasmic
68 C-ring is the flagellar rotor and the target for functional regulation by the chemotaxis
69 machinery; (iii) a hollow rod anchored to the MS-ring spans the cell envelope, connecting
70 the basal body with and transmitting rotation to the outer components of the flagella; (iv) the
71 double LP ring is bound to the peptidoglycan and outer membrane and acts as bushings for
72 smooth rotation of the rod; finally, (v) the in-built flagellar type III secretion system (fT3SS)
73 provides the functions necessary for the export of flagellar proteins through the flagellum
74 itself. Associated to the periphery of the flagellar basal body, the stator complex fuels
75 flagellar rotation by coupling inward proton or sodium transport to the generation of torque
76 (Chevance and Hughes, 2008; Terashima *et al*., 2008). As documented thoroughly in

77 *Escherichia coli* and *Salmonella*, flagellar assembly is sequential, with the inner components
78 of the basal body being assembled first, followed by components of the rod, LP ring and
79 hook, which cannot be exported until the functional fT3SS is completed. Subsequent
80 assembly of the filament proteins is preceded by a shift in fT3SS specificity triggered by
81 completion of the hook structure. Finally, the accessory stator and chemotaxis complexes
82 are assembled. The structure and assembly of the flagella have been reviewed thoroughly
83 elsewhere (Altegoer *et al*., 2014; Chevance and Hughes, 2008; Evans *et al*., 2014).

84 Gram-negative bacteria differ with respect to the number of flagella, their distribution
85 across the surface and the transcriptional organization and regulation of the flagellar genes.
86 Although flagellar genes are scattered in the genomes of some organisms, most often they
87 are grouped in one or a few genomic regions (Smith and Hoover, 2009). *Pseudomonas*
88 *putida* is a well-studied soil bacterium endowed with extraordinary metabolic versatility that
89 has become a model organism for biodegradation of organic toxicants and an attractive
90 platform for biofilm-based industrial applications (Gross *et al*., 2007; Li *et al*., 2007; Martins
91 Dos Santos *et al*., 2004). *P. putida* shows lophotrichous flagellation, consisting of a tuft of 5
92 to 7 flagella at a single pole (Harwood *et al*., 1989). In the reference strain KT2440, most
93 structural components of the flagella, the core chemotaxis signal transduction system and a
94 number of dedicated regulatory proteins are encoded in a ~70 kbp chromosomal region
95 known as the flagellar cluster (**Fig. 1A**). Additional genes encoding a second stator complex
96 (Toutain *et al*., 2005), several paralogs of the core chemotaxis components (García-Fontana
97 *et al*., 2013) and a set of 27 chemotaxis chemoreceptors (Corral-Lugo *et al*., 2016) are
98 scattered elsewhere in the genome.

99 The biosynthesis of bacterial flagella is a complex and ordered process that mirrors
100 the assembly sequence (Smith and Hoover, 2009). In order to achieve the correct temporal
101 regulation of flagellar genes so that the structural protein are produced as they are required
102 for assembly of the nascent flagellum, bacteria use hierarchically organized regulatory
103 circuits in the form of a transcriptional cascades (Smith and Hoover, 2009). Little is known

104 about the transcriptional organization and regulation of the flagellar genes in most members
105 of the genus *Pseudomonas*, and much of it has been extrapolated from the transcriptional
106 cascade of *Pseudomonas aeruginosa* described in the seminal work of Dasgupta *et al*.
107 (2003)**.** In this organism, the flagellar genes are organized into four classes to reflect the
108 timing of their expression and the transcription factors involved in their regulation. Class I
109 genes, encoding the master regulator FleQ and the flagellar σ factor FliA, stand at the top
110 of the hierarchy and are not regulated by any of the dedicated flagellar transcription factors.
111 Class II genes encode the cytoplasmic and membrane-bound components of the basal
112 body, the fT3SS, the two-component system FleSR and the auxiliary regulatory proteins
113 FleN and FlhF, involved in control of the number and polar location of the flagella,
114 respectively. Genes in this class are activated by FleQ in a σ^{54}-dependent fashion. Class III
115 genes encode the structural components of the rod, the outer LP ring and the hook, and
116 their expression is also σ^{54}-dependent and activated by FleR. Finally, Class IV genes,
117 encoding the filament proteins, the core components of the chemotaxis apparatus and the
118 stator complex are dependent on the flagellar σ factor FliA. In *P. aeruginosa* FleQ activation
119 of the Class II genes is antagonized by the auxiliary protein FleN and the second messenger
120 c-di-GMP (Dasgupta *et al*., 2000)**.** The histidine kinase FleS likely activates the response
121 regulator FleR by phosphorylation (Dasgupta *et al*., 2003), although the involvement of FleS
122 in flagellar gene regulation has recently been questioned (Zhou *et al*., 2021) and the signals
123 and relevant conditions have not yet been explored. FliA sequestration by the anti-σ factor
124 FlgM prevents premature activation of the Class IV promoters (Dasgupta *et al*., 2003; Frisk
125 *et al*., 2002). FliA inhibition is likely released by FlgM secretion through the fT3SS upon
126 completion of the hook, as shown first in *Salmonella* (Karlinsey *et al*., 2000), although
127 experimental evidence of this phenomenon in *P. aeruginosa* is still lacking. In addition, the
128 anti-σ factor antagonist HsbA has been shown to prvent FlgM inhibition by a partner-
129 switching mechanism. HsbA activity is in turn regulated by HsbR and HptB in response to

130 as of yet unknown signals (Bhuwan *et al*., 2012)**.** The *P. aeruginosa* flagellar system and its
131 regulation was reviewed recently (Bouteiller *et al*., 2021).

132 The *P. putida* KT2440 genome encodes all the known elements involved in flagellar
133 regulation in *P. aeruginosa*, and previous work from our group and others has confirmed the
134 role of FleQ as the master regulator of the flagellar cascade and the role of the σ factor FliA
135 activating the expression of some late flagellar genes (Blanco-Romero *et al*., 2018; Jiménez-
136 Fernández *et al*., 2016; Rodríguez-Herva *et al*., 2010; Wang *et al*., 2018). Recently, ChIP-
137 seq studies suggested that FleQ may bind *in vivo* upstream from genes encoding
138 components of the basal body (FlhA, FlhB, FlgA, FlgB, FlgF, FlgG), the hook (FliE*,* FliK),
139 the motor protein MotB, the anti-σ factor FlgM and some chemotaxis elements (CheV,
140 PP2310, PP4888) (Blanco-Romero *et al*., 2018), but the outcome of such interaction in
141 terms of transcriptional regulation has not been explored. Our recent work has clarified the
142 transcriptional organization, promoter arrangement and regulation of the *flgAMNZ* and
143 *flhAF-fleN-fliA* operons (Navarrete *et al*., 2019; Wirebrand *et al*., 2018). Nevertheless, an
144 integrated model of the *P. putida* flagellar cascade comparable to that of *P. aeruginosa* is
145 as of yet unavailable.

146 The present study clarifies the transcriptional organization of the flagellar cluster and
147 the regulatory circuit controlling flagellar synthesis in *P. putida*. Our results support a
148 transcriptional circuit in which the temporal regulation of the flagellar components is
149 achieved by the combination of a three-tier transcriptional cascade and several feedback
150 and feed-forward loops to fine-tune gene expression according to the assembly status and
151 relevant physiological and environmental cues.

152

153 **RESULTS**

154 **A cluster of 59 flagella-related genes is highly conserved in *Pseudomonas* spp.**

155 In order to identify the complete set of genes related to flagellar motility and chemotaxis
156 within the flagellar cluster, we have revised the annotation in the light of recent experimental
157 evidence. ORF PP_4328 encodes a protein of unknown function showing similarity to the
158 hook length control protein FliK. Transcription from the upstream promoter region is
159 dependent on the flagellar σ factor FliA in *P. putida* (Jiménez-Fernández *et al*., 2016)**.**
160 Accordingly, we have designated this ORF *fliK2*. The ORF immediately downstream,
161 PP_4329, is an ortholog of *flhX*, a gene identified in several bacterial genomes whose
162 product resembles the C-terminal domain of the fT3SS protein FlhB (Pallen *et al*., 2005). A
163 function of FlhX as a partial replacement for FlhB function has been documented in
164 *Helicobacter pylori* (Smith *et al*., 2009; Wand *et al*., 2006). PP_4331 encodes an ortholog of
165 *Vibrio cholerae* FlrD, an auxiliary protein to transcriptional regulation by FlrBC, the *V.*
166 *cholerae* counterparts of *Pseudomonas* FleSR (Moisi *et al*., 2009)**.** Similarly, PP_4333 and
167 PP_4334 encode orthologs of the *Vibrio* spp. ParP and ParC proteins, required for polar
168 localization of the chemotaxis complexes (Ringgaard *et al*., 2018). Finally, PP_4362,
169 PP_4363 and PP_4364 encode orthologs of *P. aeruginosa* HptB, HsbR and HsbA, involved,
170 along with the anti-sigma factor FlgM, in posttranslational regulation of FliA (Bhuwan *et al*.,
171 2012). Our results suggest that at least 59 of the genes present in the cluster are potentially
172 related to the flagellar function (**Fig. 1A; Supplementary Table S1**). In contrast, we have
173 been unable to establish such functional relationship for the seven consecutive ORFs
174 (PP_4345 to PP_4350 and PP_5673) with unusually low G+C content located upstream
175 from *flhA*, or for the single ORFs PP_4330, PP_4379 and PP_4387 (**Fig. 1A**).

176 We have examined the conservation of the flagellar cluster in 550 genomes available
177 online at the *Pseudomonas* Genome Database (Winsor *et al*., 2016); available at
178 pseudomonas.com). Precomputed ortholog analyses revealed that 51 of the genes were
179 conserved in all the genomes analyzed, 7 were conserved in over 90% of the genomes, and

180 a single gene, *fliT,* for which members of two separate ortholog groups were found, was
181 conserved in 80% of the genomes. High conservation of the 59-gene set likely suggests that
182 it encodes an integral part of the flagellar apparatus in the vast majority of members of the
183 genus *Pseudomonas*. Synteny analysis performed on 401 of the genomes revealed nearly
184 universal conservation of the gene order and orientation of the flagellar cluster, with very
185 few exceptions (complete analysis in **Supplementary File S1**). Based on the chromosomal
186 location of the flagellar cluster genes, we have defined four groups encompassing most of
187 the genomes analyzed (**Fig. 1B; Supplementary File S1**). In Group I, including multiple *P.*
188 *putida* and *Pseudomonas syringae* strains among others, all genes are found in a single
189 chromosomal region in the same order and orientation as in *P. putida* KT2440. Group II,
190 including strains of *Pseudomonas fluorescens* and related species, bears the flagellar
191 cluster split in two separate regions, with the split point between *flgF* and *flgE*. Exceptionally,
192 the *fliK2-flhX* gene pair was not linked to the cluster in some members of groups I and II
193 (e.g., *P. syringae* and *Pseudomonas savastanoi* strains) In Group III, which includes most
194 *Pseudomonas stutzeri* strains examined, the cluster is disrupted between *fliC* and *flgL*, and
195 in ~70% of the cases, also between *fleQ* and *fliT*, resulting in the location of their flagellar
196 clusters in two or three separate chromosomal regions. Finally, Group IV, encompassing
197 most *P. aeruginosa* strains, displays the only major disruption in the synteny of the cluster:
198 the genes *hptB*, *hsbR* and *hsbA* are found downstream from *cheR* in one chromosomal
199 location, while segments containing *fliK2* to *fliK* and *fliJ* to *flgB* are located in two additional
200 chromosomal regions. A similar analysis revealed that orthologs of *motA* and *motB*, the only
201 structural flagellar genes not linked to the *P. putida* flagellar cluster, are present in nearly all
202 the *Pseudomonas* genomes analyzed, in a separate chromosomal location, in the order
203 *motAB*, and almost invariably linked to the gene *rsgA* and the orthologs of the KT2440 ORF
204 PP_4906 (**Supplementary File S1**).

205 Flagellar clusters generally include additional genes; some are related to covalent
206 modification of the flagella or are the result of duplication of specific genes in the cluster (

207 Dasgupta *et al*., 2003), while others appear unrelated to flagellar function. Synteny analysis
208 also revealed that insertion of additional genes occurs preferentially at some of the split
209 points noted above (*flhB2-flrD*, *hsbA-fliJ*, *fliC-flgL*, *flgF-flgE* and *flgB-cheR*), along with the
210 *flhA-flhB* and (less commonly) the *fliE-fleR* intergenic region (**Fig. 1B; Supplementary File**
211 **S1**).

212 Taken together, the results of our analysis suggest that *Pseudomonas* genomes have
213 evolved to preserve the sequence and organization of a set of 59 genes related to the
214 flagellar function. Accordingly, most genes in the cluster are found in the same genomic
215 neighborhood in all the genomes analyzed, and disruption of synteny occurs almost
216 exclusively in a few specific locations.

217 **Transcriptional organization of the *P. putida* KT2440 flagellar cluster**

218 As a first approach to the identification of the transcriptional units present at the
219 KT2440 flagellar cluster, we analyzed the coverage obtained in a strand-specific RNA-seq
220 experiment (**Fig. 2A, C and E**). We observed continuous, uninterrupted strand-specific
221 transcription, as expected for genes co-transcribed as an operon, in ten regions containing
222 flagellar genes within the cluster: *fliK2-flhB2* and *flgAMNZ* at the top strand, and *flhAF-fleN-*
223 *fliA-cheYZAB-motCD-parCP-cheW-flrD*, *hsbAR-hptB-fliKLMNOPQR-flhB*, *fliHIJ*, *fliEFG*,
224 *fliC-flaG-fliDST-fleQSR*, *flgFGHIJKL*, *flgBCDE-pp4387*, and *cheV-cheR* at the bottom
225 strand. Continuous bottom strand transcription was also observed at a region spanning
226 *motA* and *motB* (**Supplementary Fig. S1**). Since the neighboring genes are transcribed
227 from the top strand, these results suggest that *motA* and *motB* are co-transcribed as a
228 bicistronic operon.

229 In contrast to our RNA-seq results, the fourteen-gene string running from *flhA* to *flrD* is
230 broken into seven separate transcriptional units in *P. aeruginosa* (Dasgupta *et al*., 2003).
231 On the other hand, our recent work showed that at least *flhA*, *flhF*, *fleN* and *fliA* are part of
232 the same operon in *P. putida* (Navarrete *et al*., 2019). To test the validity of the transcriptional
233 organization inferred from the RNA-seq data, we performed RT-PCR with oligonucleotides

234 framing all intergenic regions larger than 3 bp from *flhA* to *flrD* and cDNA from *P. putida*
235 KT2442, a rifampicin-resistant derivative of KT2440, as a template (**Fig. 2B**) Amplification
236 was obtained from all of the intergenic regions tested, strongly suggesting that transcripts
237 initiated from P*flhA* span all fourteen coding regions down to *flrD*. This assay was also
238 performed with cDNA from MRB49, a KT2442 derivative bearing a polar miniTn*5*-Km
239 insertion in *flhF* (Navarrete *et al*., 2019). Transcription levels were diminished for all
240 intergenic regions downstream from the insertion down to *motD-parC*. Polarity was not
241 observed at the *parP-cheW* and *cheW-flrD* junctions. The loss of the polar effect in this
242 region and the increased transcription obtained in both the wild-type and mutant strain,
243 suggest the presence of an internal promoter activity. We note that one or more FliA-
244 dependent internal promoters may be present in this region and not be detected in this
245 background, as polarity of the *flhF*::miniTn*5*-Km mutation renders this strain FliA$^-$ (Navarrete
246 *et al*., 2019).

247 Discrepancy with the transcriptional organization proposed for *P. aeruginosa* was also
248 observed at the regions spanning from *hptB* to *fliL*, *fliE* to *fliJ*, *fliC* to *fleR* and *flgA* to *flgZ*.
249 RT-PCR assays using KT2442 cDNA as a template and primers spanning the conflicting
250 intergenic regions confirmed co-transcription of *hptB*, *fliK* and *fliL* (**Fig.2D**) and *fliD*, *flaG*,
251 *fliD*, *fliS*, *fliT*, *fleQ* and *fleS* (**Fig. 2F**), and transcriptional termination at the *fliG-fliH* intergenic
252 region (**Fig. 2D**), consistent with the RNA-seq results. A similar RT-PCR analysis of the
253 *flgAMNZ* operon was previously published (Wirebrand *et al*., 2018). Altogether, the RNA-
254 seq and RT-PCR data and our previously published results (Navarrete *et al*., 2019;
255 Wirebrand *et al*., 2018) strongly suggest that the flagellar genes of the *P. putida* KT2440
256 flagellar cluster are transcribed as ten separate operons. In addition, at least two of the
257 operons contain internal promoters. Finally, an eleventh flagellar operon not linked to the
258 cluster spans the genes *motA* and *motB*.

259 ***P. putida* flagellar promoters revealed by sequence alignment**

260 Given the high conservation of the flagellar cluster organization across the genus
261 *Pseudomonas*, we hypothesized that such conservation may also extend to the promoter
262 regions preceding each of the operons. To test this hypothesis, we performed sequence
263 alignments of the intergenic regions upstream from *fliK2*, *flhA*, *hsbA*, *fliH*, *fliE*, *fliC*, *flgF*, *flgB*,
264 *cheV*, *flgA* and *motA*, all of which are expected to bear the primary promoters for the operons
265 defined above. For this purpose, we used the genomic sequences of *P. putida* strains
266 KT2440 and F1, *P. syringae* pv tomato strain DC3000, *P. syringae* pv syringae strain B728a,
267 *P. savastanoi* pv phaseolicola strain 1448a, *P. fluorescens* strain SBW25 and *Pseudomonas*
268 *protegens* strain Pf5 (**Fig. 3, Supplementary Fig. S2; Supplementary File S2**). While the
269 general conservation of the intergenic sequences was modest, alignments revealed
270 conserved motifs showing high similarity to the σ^{54}-dependent promoter consensus (Barrios
271 *et al*., 1999) at the intergenic regions upstream from *flhA*, *fliE*, *flgF*, *flgB* and *flgA*. We also
272 found conserved sequences bearing similar to the FliA-dependent promoter consensus
273 sequence (Rodríguez-Herva *et al*., 2010) upstream from *fliK2*, *fliC* and *cheV*, the latter
274 located within the divergent *flgA* coding sequence. A motif resembling the σ^{70}-dependent
275 promoter consensus featuring an extended -10 and a poor -35 box (Bown *et al*., 1997) was
276 present upstream from *hsbA*. We observed that the intergenic region upstream from *fliH* was
277 too short to accommodate a promoter (<15 bp) in the *P. fluorescens*, *P. protegens*, *P.*
278 *syringae* and *P. savastanoi* strains used in the alignment. A survey of *P. putida* strains
279 revealed generally longer intergenic regions containing two copies of a repetitive extragenic
280 palindromic sequence previously documented (Aranda-Olmedo *et al*., 2002), but no obvious
281 similarity to known promoter consensus motifs. Yet, as our RNA-seq and RT-PCR results
282 predict that a promoter must be active upstream from *fliH*, we included this region in the
283 analyses below.

284 Because we have previously shown evidence of the presence of additional promoter
285 activities upstream of *flhF*, *fliS* and *flgM* (Jiménez-Fernández *et al*., 2016; Navarrete *et al*.,
286 2019; Wirebrand *et al*., 2018), we also assessed the presence of putative promoter motifs

287 by means of sequence alignment in multiple additional intergenic regions of the flagellar
288 cluster (**Fig. 3, Supplementary Fig. S2; Supplementary File S2**). Additional matches to
289 the σ^{54}-dependent promoter consensus were identified at the intergenic regions upstream
290 from *fliL*, *fliK* and *fleS*, while sequences showing conservation at the -24 but not the -12 motif
291 were found upstream from *fliD and flgZ*. We also identified conserved sequences matching
292 the FliA-dependent promoter consensus upstream from *fliS* and *flgM*, and a putative σ^{70}-
293 dependent promoter motif upstream from *fleQ*. Finally, putative internal promoters located
294 within the coding sequences of the preceding genes were also found upstream from *parC*
295 and *flhF* (σ^{54}-dependent), and *cheA* (FliA-dependent) In summary, this analysis revealed
296 twenty-one putative flagellar promoters. Twelve such regions bear matches to the σ^{54}
297 consensus, seven show similarity with the FliA consensus, and two more harbor putative
298 σ^{70} promoter motifs.

299 **Strategy for analysis of the regulation of the *P. putida* flagellar cluster promoters**

300 In order to characterize the expression from the putative flagellar promoters identified,
301 we expanded our pre-existing collection of *P. putida* promoter fusions (Jiménez-Fernández
302 *et al*., 2016) to include all the potential promoter regions identified. The selected regions
303 were cloned into the Gateway® vectors pMRB2 or pMRB3 to generate transcriptional fusions
304 to the reporters *gfp*-mut3 and *lacZ*, as previously described (Jiménez-Fernández *et al*.,
305 2016). All twenty-two *gfp-lacZ* fusion plasmids and the empty vector control pMRB1 were
306 transferred to selected *P. putida* strains by mating. Expression was subsequently monitored
307 along the growth curve by means of A_{600} and GFP fluorescence measurements in a
308 microtiter plate reader with temperature and shaking control capabilities. GFP fluorescence
309 was plotted *vs* A_{600} and differential rates of GFP accumulation during exponential growth
310 ($d\mathit{fluorescence}/dA_{600}$) were calculated from the slope of the linear fit of the plotted data
311 (Jacob and Monod, 1961) (**Supplementary Fig. S3**).

312 To assess the effect of different regulatory factors on flagellar/chemotaxis promoter
313 transcription we used a subtractive approach in which we compared activity of the gene
314 fusion constructs in the wild-type strain with that in mutants bearing deletions of single
315 regulatory genes in an otherwise wild-type background. To this end, we chose the wild-type
316 *P. putida* strain KT2442 and its mutant derivatives MRB52, MRB149, MRB71 and MRB93,
317 bearing in-frame deletions of the *fleQ*, *rpoN*, *fleN* and *fleR* regulatory genes, respectively.
318 To assess whether the observed regulatory effects are direct or indirect, we used an additive
319 strategy. To this end, we constructed MRB130, a *P. putida* KT2442 derivative lacking the
320 flagellar cluster (Δflagella), including all the regulatory elements therein. In this background,
321 we inserted miniTn*7* derivatives expressing regulatory elements ectopically to test their
322 effect on the expression of the fusion constructs of the flagellar/chemotaxis predicted
323 promoter regions in the absence of other components of the flagellar cascade. In this
324 context, we interpreted restoration of expression in the presence of FleQ or FliA as evidence
325 of direct interaction between each regulatory factor and the cognate promoter region.

326 **P*fleQ* and P*fliH* transcription is not regulated by FleQ, FleR or FliA.**

327 Analysis of the differential rates of GFP accumulation from the P*fleQ-gfp-lacZ* and
328 P*fliH-gfp-lacZ* fusions revealed low expression levels (4.06±0.30 and 5.45±0.26 arbitrary
329 units, respectively), indistinguishable from to the empty vector values (3.88±0.42 arbitrary
330 units). As an alternative approach, expression was monitored by end-point β-galactosidase
331 assays in exponential and stationary phase. Expression from both promoters was negligible
332 in exponential phase, but the activity levels were substantially increased (4- to 5-fold) in
333 stationary phase (**Fig. 4**). P*fleQ* and P*fliH* transcription was not significantly altered in strains
334 lacking the transcription factors FleQ and FleR, or the auxiliary regulatory protein FleN.
335 Using the additive approach we noted that the P*fleQ* fusion activity was 2-fold lower in the
336 Δflagella strain in stationary phase. However, the wild-type expression levels were not
337 restored by ectopic production of FleQ or FliA (**Fig. 4A**). P*fliH* expression was not affected
338 by the deletion of the complete flagellar cluster or the ectopic production of FliA (**Fig. 4B**).

339 Taken together, these results suggest that the upstream regions of *fleQ* and *fliH* contain
340 promoters that are poorly expressed in exponential phase, induced in stationary phase, and
341 not significantly regulated by any of the known flagellar transcription factors.

342 **Twelve flagellar promoters are directly regulated by FleQ**

343 Analysis of the differential rates of GFP accumulation showed that all twenty additional
344 flagellar promoters drove significant levels of transcription from the fusion constructs (**Figs.**
345 **5 and 6)**. Fifteen of these fusions were clearly downregulated (2- to 41-fold) in the Δ*fleQ*
346 strain, suggesting the direct or indirect involvement of FleQ in their regulation. Statistically
347 significant regulation below the 2-fold threshold was also observed for the weakly active
348 P*fliK*, P*fliD* and P*flgZ* promoter regions, and for P*flhF* and P*hsbA*, which showed relatively
349 high levels of FleQ-independent expression. Taken together, our results are fully consistent
350 with the notion that FleQ is the master activator of the synthesis of the vast majority of
351 flagellar and chemotaxis components.

352 To identify which flagellar promoters are directly regulated by FleQ, we tested the
353 expression of the set of FleQ-activated promoter fusions in the Δflagella strain bearing
354 miniTn*7-nahR*-P*sal-fleQ*, which produces FleQ ectopically from the salicylate-inducible P*sal*
355 promoter (**Figs. 5 and 6**). Preliminary assays showed that salicylate induction greatly
356 decreased the growth rate and was not used in these experiments. Nevertheless, ectopic
357 production of FleQ from uninduced P*sal* was sufficient to cause a great increase in
358 expression (7- to 110-fold) from the P*parC*, P*flhF*, P*flhA*, P*fliL*, P*fliK*, P*fliE*, P*fleS*, P*fliD*, P*flgF*,
359 P*flgB* and P*flgA* promoter fusions. Activity of the weak P*flgZ* was also increased (<2-fold) by
360 ectopic expression of FleQ. These results suggest that FleQ interacts directly with these
361 twelve promoter regions to activate transcription. All of these promoter regions were
362 predicted to bear putative σ^{54}-dependent promoters based on the alignments shown above.
363 Consistently, all fusions in this set showed reduced expression in the Δ*rpoN* background
364 (**Fig. 5**), with the only exception of the P*fliD* construct, which harbors only a partial match to
365 the σ^{54} consensus (also see below).

366 Expression from the twelve FleQ-activated fusions was also measured in a KT2442
367 derivative lacking the auxiliary regulatory protein FleN (**Fig. 5**). Fluorescence accumulation
368 from eleven of the twelve fusions was clearly increased (2- to 13-fold) in the Δ*fleN*
369 background. Exceptionally, a small (less than 2-fold) but statistically significant increase was
370 observed for the weak P*flgZ* promoter. These results support the notion that FleN
371 antagonizes FleQ activation of the flagellar promoters (Dasgupta and Ramphal, 2001). The
372 second messenger c-di-GMP has been shown to positively and negatively modulate FleQ
373 activity (Baraquet *et al*., 2012; Claudine and Harwood, 2013; Hickman and Harwood, 2008).
374 We also tested expression of the twelve fusions in *P. putida* strains that produce the
375 diguanylate cyclase PleD* or the phosphodiesterase YhjH ectopically, thus increasing or
376 decreasing the intracellular c-di-GMP concentrations. To this end, we chose a KT2442
377 derivative lacking the high molecular weight adhesin LapA, as c-di-GMP overproduction
378 provokes aggregation of LapA$^+$ *P. putida* (Jiménez-Fernández *et al*., 2016) that precludes
379 accurate absorbance and fluorescence measurements. Artificially decreasing the
380 intracellular c-di-GMP concentration led to expression levels comparable to those in the
381 unmodified wild-type strain in all cases (**Fig. 5**), suggesting that c-di-GMP levels are
382 naturally low under our experimental conditions. In contrast, all twelve fusions were
383 downregulated (2- to 20-fold) in the presence of high c-di-GMP levels. Taken together, our
384 results indicate that the P*parC*, P*flhF*, *flhA*, P*fliL*, P*fliK*, P*fliE*, P*fleS*, P*flgF*, P*flgB* and P*flgA*
385 promoters are dependent on the alternative σ factor σ^{54}, positively regulated by FleQ,
386 negatively regulated by FleN and inhibited by high c-di-GMP levels. Although we have not
387 been able to detect the σ^{54} dependence of P*fliD* coincidence of its behavior with the rest of
388 the set in every other regard suggest that this may be a limitation of the technique due to
389 the low expression levels of this promoter. Finally, P*flgZ*, another poorly expressed
390 promoter, exhibited a similar response to FleQ, FleN, σ^{54} and c-di-GMP, but the extent of
391 the regulation was modest in all cases.

392 **FleR is not essential for flagellar function and flagellar gene expression**

393 The FleSR two-component system is responsible for the activation of Class III flagellar
394 genes in *P. aeruginosa* and other bacteria (Dasgupta *et al*., 2003; Echazarreta and Klose,
395 2019), but is not characterized in *P. putida*. To explore a possible function of FleSR in
396 flagellar motility and the regulation of the flagellar cluster, we constructed MRB92 and
397 MRB93, two KT2442 derivatives bearing in-frame deletions of *fleS* and *fleR*, respectively.
398 Swimming assays were performed with the Δ*fleR* and Δ*fleS* mutant using the wild-type and
399 Δ*fleQ* strains as positive and negative controls, respectively. The sizes of the swimming
400 halos produced by the wild-type, Δ*fleR* and Δ*fleS* strains were indistinguishable, while no
401 motility halo was obtained with the Δ*fleQ* mutant (**Supplementary Fig. S4**). These results
402 indicate that FleR and FleS are not essential for flagellar motility, at least under our
403 experimental conditions.

404 To determine the contribution of FleR to the regulation of the flagellar promoters,
405 expression from the fusion set was also examined in the Δ*fleR* mutant (**Figs. 5 and 6**).
406 Deletion of *fleR* had little or no significant effect on most flagellar promoters. However, a
407 modest decrease in expression above the two-fold threshold was observed for the FleQ-
408 dependent P*parC*, P*flgF* and P*flgB* promoters. These results suggest that FleR does not
409 have a major role in the regulation of flagellar gene expression, but may contribute to fine-
410 tune the expression of some flagellar operons.

411 **Eight flagellar promoters are directly regulated by FliA**

412 The additive approach was also used to assess which promoters of the flagellar cluster
413 are directly regulated by the flagellar σ factor FliA. To this end, expression of the complete
414 set of FleQ-regulated flagellar promoters was assessed in the Δflagella strain bearing
415 miniTn*7-nahR*-P*sal-fliA*, which produces FliA ectopically from the salicylate-inducible P*sal*
416 promoter. As with the FleQ-producing construct above, salicylate induction was detrimental
417 to growth, but in the absence of salicylate, ectopic production of FliA stimulated expression
418 (4- to 33-fold) from all seven promoter regions (namely P*fliK2*, P*cheA*, P*fliS*, P*fliC*, P*cheV*,
419 P*flgM* and P*motA*) bearing matches to the FliA consensus sequence (**Fig. 6**). Ectopic

420 production of FleQ failed to alter the expression from any of these fusions, except for a
421 modest (2-fold) increase in P*fliK2* (**Fig. 6**). Conversely, ectopic production of FliA had little
422 or no effect (≤2-fold) on the expression of the twelve FleQ-regulated promoters above (**Fig.**
423 **5**). Although the FliA-dependent fusions were generally downregulated in the Δ*fleQ*, Δ*rpoN*
424 and Δ*fleN* backgrounds, P*fliC* expression was increased in the absence of FleN (**Fig. 6**).
425 Taken together, our results suggest that the promoters contained at the P*fliK2*, P*cheA*, P*fliS*,
426 P*fliC*, P*cheV*, P*flgM* and *motA* promoter regions are dependent on the alternative σ factor
427 FliA, and indirectly regulated by σ^{54} and FleQ. An additional promoter region not carrying an
428 evident match to the FliA consensus, P*hsbA*, showed a similar response pattern to FliA,
429 FleQ and σ^{54}, but the extent of the regulation was 2-fold or less in all cases and significant
430 basal transcription was observed in all backgrounds. We propose that this promoter region
431 may contain a weak, previously undetected FliA-dependent promoter and an additional FliA-
432 independent promoter activity.
433

DISCUSSION

The *P. putida* KT2440 flagellar cluster resides in a ~70 kbp chromosomal region encoding the vast majority of structural and regulatory flagellar proteins along with the core components of the chemotaxis machinery. Here we expand on our previous work (Jiménez-Fernández *et al*., 2016; Navarrete *et al*., 2019; Wirebrand *et al*., 2018) to identify the transcriptional organization of the *P. putida* KT2440 flagellar cluster and characterize the transcriptional regulation of twenty primary and internal promoters accounting for the expression of all but three relevant . The results presented provide (i) updated annotations and putative functions for seven flagellar genes; (ii) evidence of the transcriptional organization of the flagellar cluster in ten separate operons, while an additional operon, *motAB*, is not linked to the cluster; (iii) an inventory of twenty-two flagellar promoters, including eleven primary and eleven internal promoters; (iv) characterization of the regulation of all twenty-two flagellar promoters regarding their dependence on known flagellar transcription factors (FleQ, FleR, FliA, σ^{54}), the auxiliary protein FleN and the intracellular signalling molecule c-di-GMP; (v) a novel hierarchy for the transcriptional cascade controlling flagellar gene expression that differs significantly from those previously described; (vi) evidence of high conservation of the flagellar gene complement and organization in the genus *Pseudomonas*; and (vii) evidence of high conservation of the flagellar promoter motifs in a set of environmental *Pseudomonas*, suggesting that many of the results presented here may be applicable to this group of organisms.

We have defined the *P. putida* KT2440 flagellar cluster as the chromosomal region encompassing ORFs PP_4328 (*fliK2*) to PP_4397 (*flgZ*). These boundaries were established based on three lines of evidence. (i) High conservation: 51 of the flagellar genes are present in all the *Pseudomonas* genomes analyzed; the remaining 8 are found in at least 80%; (ii) conservation of gene arrangement: all flagellar genes are clustered in the same order in one to three chromosomal locations in most *Pseudomonas* genomes analyzed (**Supplementary File 1**); and (iii) experimental evidence of involvement in flagellar function:

all but one of the 59 flagellar genes in the cluster have been demonstrated to play roles related to assembly and operation of the flagellar and chemotaxis complexes in at least one organism. In addition to the genes previously annotated, we have been able to identify an ortholog to *H. pylori flhX*, encoding a small protein similar to the processed form of FlhB that determines the specificity switch of the fT3SS (Pallen *et al*., 2005). FlhX has been shown to partially complement FlhB function in *H. pylori* (Smith *et al*., 2009), but its actual role in flagellar assembly is not well understood. One more gene in the cluster is an ortholog of *V. cholerae flrD*, encoding a transmembrane signal transduction protein that stimulates transcriptional activation by the FlrBC two-component system (equivalent to FleSR) (Moisi *et al*., 2009). We have also identified orthologs of *Vibrio* spp. *parP* and *parC*, encoding two polar landmark proteins required for polar positioning of the chemotaxis arrays (Ringgaard *et al*., 2018). Finally, we have annotated the orthologs of *P. aeruginosa hptB*, *hsbR* and *hsbA*, encoding a phosphotransferase a response regulator and an anti-σ factor antagonist proteins. This system antagonizes FlgM sequestration of FliA by partner-switching mechanism (Bhuwan *et al*., 2012) and indirectly regulates biofilm formation by regulating the activity of the diguanylate cyclase HsbD (Valentini *et al*., 2016). In contrast, the function of *fliK2* is still uncharacterized. However, because *fliK2* is part of an operon with *flhX*, and its transcription is FliA-dependent in *P. putida*, we find it likely that it will eventually demonstrate to be a *bona fide* flagellar gene. With the updated annotation, we conclude that the conserved *Pseudomonas* flagellar cluster gene set encodes all the structural proteins of the flagellum (minus an additional flagellar motor encoded by the *motAB* operon elsewhere), all the elements required for flagellar assembly (including the complete fT3SS), all the core components of the chemotaxis apparatus, three dedicated transcription factors, seven auxiliary proteins to control their activity, three landmark proteins for the polar location of the flagellar and chemotaxis complexes, and one protein involved in functional regulation of flagellar rotation (**Supplementary Table 1**). We note that, in addition to the conserved gene

complement described here, some organisms bear species- or strain-specific flagellar genes in their clusters [e.g., genes for flagellin glycosylation (Dasgupta *et al*., 2003)].

The *P. putida* KT2440 flagellar cluster is organized in ten transcriptional units, with primary promoters located upstream from *fliK2*, *flhA*, *hsbA*, *fliH*, *fliE*, *fliC*, *flgF*, *flgB*, *cheV* and *flgA*. In addition, internal promoters are found upstream from *flhF*, *cheA* and *parC* at the *flhAF-fleN-fliA-cheYZAB-motCD-parCP-cheW-flrD* operon, upstream from *fliK* and *fliL* at the *hsbAR-hptB-fliKLMNOPQE-flhB* operon, upstream from *fliD*, *fliS*, *fleQ* and *fleS* at the *fliC-flaG-fliDST-fleQRS* operon and upstream from *flgM* and *flgZ* at the *flgAMNZ* operon (**Fig. 2**). Some of the promoters shown here were identified and partially characterized in our previous work (Jiménez-Fernández *et al*., 2016; Navarrete *et al*., 2019; Wirebrand *et al*., 2018)**.** Our results indicate that much of the *P. putida* KT2440 flagellar cluster is transcribed as part of long operons containing internal promoters. The recent development of high throughput RNA-sequencing techniques with the possibility of genome-wide mapping of transcriptional start and termination sites has revealed that nested operon architectures are much more common in bacterial genomes than expected (Conway *et al*., 2014; Vera *et al*., 2020; Warrier *et al*., 2018; Yan *et al*., 2018).

While the operon arrangement described here is generally reminiscent to that proposed for *P. aeruginosa* (Dasgupta *et al*., 2003), the *P. aeruginosa* cluster does not contain any operons with a nested architecture. Rather, the genes are grouped in shorter transcriptional units. We observe that the *P. aeruginosa* counterparts to the internal promoters shown here are regarded as primary promoters, which leads to the division of these operons into shorter transcriptional units. Whether this is the result of interspecies differences within *Pseudomonas* or a consequence of the different approaches used to characterize the transcriptional organization of these genes remains to be determined. However, it is noteworthy that long, nested flagellar operons have been described in other polarly-flagellated Gamma-proteobacteria (Y. K. Kim and McCarter, 2000; Prouty *et al*., 2001; Wilhelms *et al*., 2011; Wu *et al*., 2011).

The regulatory architecture of the flagellar transcriptional cascade has been elucidated in the polarly flagellated Gamma-proteobacteria *V. cholerae* (Prouty *et al*., 2001), *Vibrio parahemolyticus* (McCarter, 2001), *Vibrio campbelli* (Petersen *et al*., 2021), *Legionella pneumophila* (Albert-Weissenberger *et al*., 2010), *Aeromonas hydrophila* (Wilhelms *et al*., 2011), *Shewanella oneidensis* (Shi *et al*., 2014), *P. aeruginosa* (Dasgupta *et al*., 2003) and now *P. putida* (**Fig. 7**). Comparative analysis of the models proposed in these organisms suggests a number of common themes along with significant organism-to-organism variability even within the same genus. All the transcriptional cascades described are three- or four-tiered, with the transcription factor FleQ (also known as FlrA) at the top of the regulatory hierarchy. Accordingly, *fleQ/flrA* is invariably a Class I gene (i.e., its transcription does not require any of the dedicated flagellar transcription factors). Synthesis of FleQ/FlrA is likely activated in response to environmental and physiological cues that favor a motile lifestyle, but the conditions and regulatory mechanisms involved are generally not well understood. Regulation of *fleQ* expression in diverse *Pseudomonas* species may involve repression by the CRP ortholog Vfr (Dasgupta *et al*., 2002), AmrZ (Tart *et al*., 2006), OsaR (Ma *et al*., 2021) and activation by the AlgU-regulated antisense RNA $fleQ_{as}$ (Markel *et al*., 2018). We have found that P*fleQ* is induced in stationary phase and not regulated by FleQ, FleR or FliA, suggesting that it belongs to Class I (**Fig. 4A**). Since transcription from P*fleQ* is not interrupted at the intergenic region between *fleQ* and *fleS* (**Fig. 2E and F**), *fleQ*, *fleS* and *fleR* must be considered Class I flagellar genes in *P. putida*, even though *fleS* and *fleR* are also transcribed from their own FleQ-dependent promoter. Although we have not explored regulation of the P*fleQ* promoter further, we note that the AlgU-dependent promoter motifs for $fleQ_{as}$ are conserved in a wide range of *Pseudomonas* (Markel *et al*., 2018), and we observe significant levels of antisense transcription around the 5' end of *fleQ* coding sequence (**Fig. 2E**), suggesting that $fleQ_{as}$ may also be produced and operate in *P. putida*. A second promoter, P*fliH* driving the synthesis of the secretion ATPase components FliH, FliI and FliJ, showed a similar behavior to P*fleQ*: its expression was low in exponential

phase, induced in stationary phase and unresponsive to any of the dedicated flagellar transcriptions factors (**Fig. 4B**). Accordingly, we also classify FliH, FliI and FliJ as Class I genes. We note that the presence of additional Class I genes other than the master regulation is not uncommon in polarly flagellated Gamma-proteobacteria (Dasgupta *et al*., 2003; Petersen *et al*., 2021; Wilhelms *et al*., 2011), and *flrB* and *flrC* are actually Class I genes in *V. campbellii* (Petersen *et al*., 2021).

FleQ activation of Class II genes sets in motion the assembly of the basal body (**Fig. 7**). Polar localization of the flagella is directed by the signal recognition particle-like GTPase FlhF (Schuhmacher *et al*., 2015). FlhF is likely the first flagellar gene product to locate to the cell pole and has been shown to recruit the first assembly building block, the MS-ring structural protein FliF, in *V. cholerae* (Green *et al*., 2009). As basal body assembly progresses, the MinD-like ATPase FleN (also known as FlhG) provides a negative regulatory loop by inhibiting the ATPase activity of FleQ, required for σ^{54} promoter activation (**Fig. 7**) (Baraquet and Harwood, 2013). Deletion of *fleN* provokes hyperflagellation and *fleN* overexpression prevents the synthesis of flagella (Schuhmacher, *et al*., 2015), suggesting that it may become active in response to an checkpoint that indicates that assembly of the correct number of flagella has been initiated. Recently, Blagotinsek *et al*., (2020) showed that FlhG is recruited to the flagellar pole as an inactive monomer by the C-ring protein FliM in *S. oneidensis*. Membrane-bound FlhG may then undergo ATP-induced dimerization to become active in a process that is stimulated by interaction with membrane lipids (Schuhmacher *et al*., 2015). The ATP-bound dimer is the form that interacts with FleQ to prevent Class II promoter activation (Baraquet and Harwood, 2013). Thus, assembly of the C-ring(s) may be the signal that triggers FleN-dependent inhibition of Class II promoter transcription. The extent of flagellar assembly enabled by FleQ-activated transcription is most often restricted to all or part of the early basal body (EBB) structures, namely the MS-ring, the C-ring and the fT3SS (Dasgupta *et al*., 2003; Khan *et al*., 2020). In contrast, we have shown that *P. putida* Class II genes encode all structural flagellar components except

for the filament. This arrangement is reminiscent of that proposed for *V. campbellii* (Petersen *et al*., 2021) and *S. oneidensis* (Shi *et al*., 2014).

An additional tier, Class III, activated by the FleSR (also known as FlrBC) two-component system is required in *P. aeruginosa*, *V. cholerae*, *V. parahemolyticus* and *A. hydrolitica* to complete the assembly of the components of the hook-basal body (HBB) complex (Dasgupta *et al*., 2003; Khan *et al*., 2020; Wilhelms *et al*., 2011). Activation of FleSR/FlrBC was recently shown to respond to the assembly of the EBB in *V. cholerae* and *P. aeruginosa* (Burnham *et al*., 2020), as previously observed with the Epsilon-proteobacteria *Campylobacter jejuni* and *Helicobacter pylori* (Boll and Hendrixson, 2013; Tsang and Hoover, 2015). Sensing of the assembly status may be mediated by FlrD, a membrane protein containing a HAMP domain that stimulates FlrBC-dependent activation in *V. cholerae* (Moisi *et al*., 2009)**.** *P. putida* encodes orthologs of FlrD and FleSR (**Supplementary Table S1**). However, because transcription of all the HBB genes is directly dependent on FleQ, FleR is not essential for the assembly of functional flagella (**Supplementary Fig. S4**). Yet, we have shown that transcription from the P*flgB* and P*flgF* promoters, driving the synthesis of the structural rod, LP ring and hook proteins, is somewhat diminished in the Δ*fleR* strain (**Fig. 5**), and sequence alignment revealed multiple conserved sequences with high similarity to the proposed FlrC binding motif (CGGCAA) in our set of seven environmental *Pseudomonas* strains in both promoter regions (**Supplementary File 2**). These observations suggest that FleR may play an unrecognized role in the synthesis of the late basal body and hook components. Interestingly, replacement of the *V. cholerae* P*flgB*, P*flgF* and P*flgK* FlrC-dependent promoters for the FlrA-dependent P*fliE* resulted in normal flagellation and motility in the wild-type strain, but provoked the loss of the flagellum and motility in a Δ*flhG* background, suggesting that the FlrBC may provide robustness to the regulatory circuit in the event of faulty FlhG function (Burnham *et al*., 2020). Accordingly, we hypothesize that FleSR activation of the P*flgB* and P*flgF* promoters in *P. putida* may act as a safeguard against a shortage of rod and hook subunits if FleQ activation is compromised

by altered FleN signaling. While this evidently does not happen in our experimental setting, there may be conditions in which such backup activation by FleR may relevant. Overlapping functions of FleQ and FleR have been documented in a few other systems. FlrC, the FleR ortholog of *S. oneidensis*, is not required for motility and plays a minor role in the regulation of the flagellar promoters (Shi *et al*., 2014). In this organism ectopic production of FlrC can suppress the nonmotile phenotype of a Δ*flrA* mutant (lacking the cognate FleQ ortholog) by replacing FlrA as the activator of the flagellar σ^{54}-dependent promoters (Gao *et al*., 2018). In a similar vein, the functions of FlrA and FlrC are partially redundant in the flagellar cascade of *V. campbelli*; however, in this case, it is FlrA, and not FlrC, that is dispensable for flagellar motility (Petersen *et al*., 2021). Finally, in *Rhodobacter sphaeroides*, FleQ and the FleR ortholog FleT cooperate in the regulation of Class III flagellar promoters by forming a heterooligomeric protein (Poggio *et al*., 2005). These and other possibilities of interplay between the two *P. putida* σ^{54}-dependent activators are worth exploring in the future.

The final tier in the flagellar cascades is triggered by the release of FliA from inactivation by the anti-σ factor FlgM. As first demonstrated in *Salmonella*, a shift in secretion specificity upon completion of the hook structure leads to FlgM secretion by way of the fT3SS (Karlinsey *et al*., 2000). This is generally considered to be a conserved mechanism to activate FliA-dependent transcription in an assembly checkpoint-dependent fashion, and has been directly demonstrated in *V. cholerae* (Correa *et al*., 2004). In addition, the *P. aeruginosa* anti-sigma factor antagonist HsbA has been show to prevent FlgM-dependent inactivation of FliA by a partner-switching mechanism in response to a phosphorylation cascade involving several membrane hybrid sensor kinases, the histidine phosphotransferase HtpB and the response regulator HsbR (Bhuwan *et al*., 2012), but the signals triggering this system are currently not known and its connection with flagellar assembly is therefore unclear. As the *P. putida* flagellar cluster encodes FlgM, HsbA, HsbR and HtpB orthologs (**Supplementary Table S1**), any of these mechanisms may be

functional, but we have not explored them in this work. The set of FliA-dependent Class IV genes in polarly flagellated Gamma-proteobacteria normally includes flagellin and other filament components, along with chemotaxis and flagellar stator genes. In *P. putida* FliA is essential for expression of *fliC* and *flaG*, encoding flagellin and a regulator of filament length, the chemotaxis operon *cheVR*, the stator genes *motAB* and the uncharacterized *fliK2-flhX* operon (**Figs. 2, 5, 6 and 7**), and boosts transcription of the distal chemotaxis and stator genes of the Class II *flhAF-fleN-fliA-cheYZAB-motCD-parCP-cheW-flrD* operon. Accordingly, FliA is essential for assembly of the filament and completion of the chemotaxis signal transduction system and one of the stator complexes (**Fig. 7**). We note that, although the core chemotaxis and the *motCD* stator genes were previously assigned to Class IV in *P. aeruginosa* (Dasgupta *et al*., 2003), re-examination of the evidence revealed that none of the orthologs of the *flhAF-fleN-fliAcheYZAB-motCD-parCP-cheW-flrD* operon genes were significantly downregulated in a Δ*fliA* mutant, and should therefore be re-classified as Class II [(see Supplementary Tables 2-6 in Dasgupta *et al*. (2003)]

FliA also participates in feed-forward and feedback loops on several regulatory elements (**Fig. 7)**: it boosts the synthesis of the anti-sigma FlgM and the HsbA-HsbR-HptB system (**Fig. 6**), which possibly provides an alternative pathway to relieve FliA sequestration in response to unknown signals (Bhuwan *et al*., 2012). Most intriguingly, FliA-dependent transcription of *fleQ* and *fleSR* as part of the *fliC-flaG-fliDST-fleQSR* operon (**Fig. 2**) provides positive feedback to the synthesis of the transcription factors involved in early flagellar gene expression (**Fig. 7**). Since FleQ function and Class II transcription may be transiently impaired by the formation of an inactive complex with FleN (Baraquet and Harwood, 2013), FleQ newly synthesized by way of readthrough transcription from the strong Class III P*fliC* promoter may titrate out FleN, restoring expression of the Class II genes. Unlike peritrichous flagellates, in which new flagella can be continuously added during cell elongation, polar flagellates such as *P. putida* must assemble their flagella in a discontinuous fashion, as a new pole is generated only once per cell cycle during cell division. New flagella must then

be assembled at the new pole in time for their completion at the following cell division. In this scenario, the reactivation of early flagellar gene expression by this FliA-mediated positive feedback mechanism appears to be a suitable mechanism to enable *de novo* flagella synthesis at the new pole while assembly at the old pole is completed.

EXPERIMENTAL PROCEDURES

Bacterial strains and growth conditions

The bacterial strains used in this work are summarized in **Supplementary Table S2.** Liquid cultures of *E. coli* and *P. putida* strains were routinely grown in Luria-Bertani (LB) broth (Sambrook and Russell, 2000) at 37°C and 30 °C, respectively, with 180 rpm shaking. For fluorescence monitoring, 1/10 strength LB was used to minimize background fluorescence. For solid media, Bacto-Agar (Difco) was added to a final concentration of 18 g l^{-1}. Antibiotics and other additions were used, when required, at the following concentrations: ampicillin (100 mg l^{-1}), carbenicillin (0.5 g l^{-1}), kanamycin (25 mg l^{-1}), rifampicin (10 mg l^{-1}), chloramphenicol (15 mg l^{-1}), gentamycin (10 mg l^{-1}), tetracycline (5 mg l^{-1}), 5-bromo-4-chloro-3-indoyl-β-D-galactopyranoside (X-gal) (25 mg l^{-1}) and sodium salicylate (from 0.1 mM to 2 mM) All reagents were purchased from Sigma Aldrich, except for X- Gal, which was purchased from Fermentas.

Plasmid and strain construction

Plasmids and oligonucleotides used in this work are summarized in **Supplementary Table S2.** All DNA manipulations were performed following standard procedures (Sambrook and Russell, 2000). Restriction and modification enzymes were used according to the manufacturers' instructions (Fermentas, Roche and NEB) When required, blunt ends were generated using the Klenow fragment or T4 DNA polymerase. *E. coli* DH5α was used as a host in cloning procedures. All cloning steps involving PCR were verified by commercial sequencing (Secugen or Stab Vida) Plasmid DNA was transferred to *E. coli* and *P. putida* strains by transformation (Inoue *et al*., 1990), triparental mating (Espinosa-Urgel *et al*., 2000) or electroporation (Choi *et al*., 2006). Site-specific integration of miniTn7 derivatives in *P. putida* strains was performed essentially as described (Choi *et al*., 2005). The flagellar cluster and *rpoN* gene were deleted by plasmid-based gene replacement as previously described (Martínez-García and de Lorenzo, 2021). For *rpoN* deletion, 500-bp fragments flanking the respective gene were PCR-amplified with oligonucleotide pairs rpoN-fwd-

EcoRI/rpoN-overlap-Rev (upstream region) and rpoN-overlap-fwd/rpoN-rev-BamHI (downstream region), subsequently combined by overlap extension PCR and cloned via *Eco*RI and *Bam*HI restriction sites into plasmid pEMG, a Km-resistant plasmid that incorporates two I-SceI sites flanking a *lacZ*α polylinker, to yield pMRB290. For flagellar cluster deletion, the plasmid pEMG-flagella (Martínez-García *et al*., 2014) containing 750-bp upstream and 816-bp downstream of PP_4297 and PP_4329 genes respectively was used. These plasmids were mobilised by triparental mating to *P. putida* KT2442 harbouring the I-SceI expressing plasmid pSW-I (Martínez-García and de Lorenzo, 2011) The positive co-integrates were selected through PCR amplification of flanking regions and resolved through induction of the I-SceI enzyme, derived from the pSW-I plasmid using 15 mM 3-methyl benzoate (3-MB) Then, the induced culture was plated onto LB agar plates and the positive colonies were assessed for the loss of the Km resistance marker. Deletions were verified by PCR. The pSW-I plasmid was cured after successive passes of the deleted strains in LB without antibiotics.

To construct *P. putida* KT2442 derivatives with in-frame deletions of *fleN*, *fleQ* and *fleR*, upstream and downstream chromosomal regions flanking these genes were PCR-amplified with an specific oligonucleotide pairs. For *fleN* deletion, fleN-up-fwd/fleN-up-rev (upstream region) and fleN-down-fwd/fleN-down-rev (downstream region) For *fleQ* deletion, fleQ-up-fwd/fleQ-up-rev (upstream region) and fleQ-down-fwd/fleQ-down-rev (downstream region) For *fleR* deletion, fleR-up-fwd-EcoRI/fleR-up-rev-BamHI (upstream region) and fleR-down-fwd-BamHI/fleR-down-rev-HindIII (downstream region) The PCR products were cleaved with EcoRI and BamHI or BamHI and HindIII, respectively, and three-way ligated into EcoRI- and HindIII- digested pEX18Tc, a gene replacement vector. A BamHI-excised FRT-flanked kanamycin resistance cassette from pMPO284 was then cloned into the BamHI site, yielding pMRB96 (*fleQ*), pMRB104 (*fleN*) and pMRB192 (*fleR*) These plasmids were transferred to *P. putida* KT2442 by electroporation. Selection of integration, allelic replacement and FLP-mediated excision of the kanamycin resistance marker was performed essentially as

described (Hoang *et al*., 1998; Llamas *et al*., 2000) to generate Δ*fleQ* (MRB52), Δ*fleN* (MRB71) and Δ*fleR* (MRB93) The structure of the deleted loci was verified by PCR.

For the construction of pMRB178 and pMRB286, plasmids producing FleQ and FliA, respectively, the *fleQ* and *fliA* open reading frames were PCR-amplified with the oligonucleotide pairs FleQ-XbaI-SD-fwd/ FleQ-SpeI-rev and FliA-fwd-XbaI-SD/FliA-rev-SpeI-Stop, digested with appropriated enzymes and cloned into XbaI- and SpeI-cleaved pMRB172, a salicylate-inducible expression plasmid bearing Tn7 transposon for site-specific genome integration.

A 750-bp fragment containing the putative P*fleS* promoter region (positions -750 to -1 relative to *fleS* start codon) was amplified using oligonucleotides PfleS-fwd/PfleS-rev as primers and cloned via SpeI and PstI restriction sites into previously cleaved pMRB196, a pMRB3-derived broad host-range *gfp*mut3::*lac*Z transcriptional fusion vector, yielding pMRB291. P*fliE* and P*flgF* 500-bp promoter regions were amplified by using oligonucleotide pairs PfliE-fwd-SpeI/PfliE-rev-PstI and PflgF-fwd-SpeI/PflgF-rev-PstI and cloned as described above to yield pMRB250 (P*flgF*) and pMRB259 (P*fliE*)

Flagellar motility (swimming) assays

Swimming assays were adapted from Parkinson (1976). Tryptone motility plates containing 0.3% Bacto-agar (Difco) were toothpick-inoculated with fresh colonies and incubated for 14 h at 30°C. At least 3 biological replicates were assayed for each strain.

***In vivo* gene expression assays**

The rates of GFP accumulation during exponential growth were used to measure gene expression in cultures bearing *gfp-lacZ* transcriptional fusions to different promoters. Overnight LB cultures of the fusion-bearing strains were diluted in 1/10 strength LB broth, and dispensed into the wells of a Costar 96 microtiter polystyrene plate (Corning) The plate was incubated in a Spark microliter plate reader/incubator at 30 °C with 510 rpm shaking to mid-exponential phase. Cultures were then diluted in the same medium and incubated in the same conditions for 23 hours. A_{600} and GFP fluorescence (485 nm excitation, 535 nm

emission) were monitored in 15-minutes intervals during incubation. Differential rates of GFP fluorescence accumulation were calculated as the slopes of the linear regression (R^2>0.98) performed on the exponential growth fluorescence vs. absorbance plots.

For β-galactosidase assays of *lacZ* fusions, overnight cultures bearing the corresponding fusion plasmids were diluted in 5 ml LB to an A_{600} of 0.01 and incubated for 24 hours at 30°C with shaking (180 rpm) Growth was then stopped, and β-galactosidase activity was determined from sodium dodecyl sulphate- and chloroform-permeabilized cells as described (Miller, 1993). Results are reported as Miller units (Miller, 1993).

RNA isolation and semi-quantitative RT-PCR

Total RNA from stationary phase cultures was extracted as described (García-González *et al*., 2005) Reverse transcription (RT) of total RNA (2 µg) was carried out using the High-Capacity cDNA Achieve kit (Applied Biosystems) following the manufacturer instructions. Amplification reactions were performed with 50 ng of cDNA as template in a 30-cycle PCR program, using appropriate oligonucleotides detailed in **Supplementary Table S2** and Illustra™ PuReTaq™ Ready-To-Go™ PCR Beads (GE Healthcare) Negative and positive controls were performed with total RNA or genomic DNA as templates, respectively. The RT-PCR products obtained were resolved by 1% agarose gel electrophoresis and visualized by ethidium bromide staining.

RNA-seq assay

5 µg of total RNA were sent to the CABIMER Genomics facility (Seville, Spain) Depletion of rRNA and preparation of cDNA libraries were carried out with the Illumina Stranded TOTAL RNA preparation RIBO-ZERO PLUS kit. Single-end sequencing was performed with the Illumina NextSeq 500 HIGH-Output flow cell and 1 x75 bp length parameters.

Bioinformatics methods

We used the pre-computed *Pseudomonas* ortholog groups available at the *Pseudomonas* genome database (Winsor *et al*., 2016) (pseudomonas.com) to assess the

conservation of the flagellar gene set in the genus *Pseudomonas*. Synteny was analyzed by computing the number of intervening genes between the orthologs of all consecutive genes in the *P. putida* flagellar cluster in all 550 genomes in the *Pseudomonas* ortholog database using a simple Microsoft Excel script and the numerical part of the Locus Tag for each pair of genes in each genome as a positional reference. The resulting dataset was manually curated and genomes yielding inconsistent or ambiguous results were discarded. A total of 401 genomes provided consistent results for the complete cluster (**Supplementary File 1**) Sequence alignment of intergenic sequences used 500 bp fragments upstream from the start codon for each gene. Occasional inconsistencies in the annotation of the start codons were corrected when required. Multiple sequence alignments were performed using MUSCLE (Edgar, 2004), available at https://www.ebi.ac.uk/Tools/msa/muscle/.

The RNA-seq raw data was pre-filtered using FASTQ Toolkit v.1.0.0. Quality of the reads was checked with FastQC (https://www.bioinformatics.babraham.ac.uk/projects/fastqc/) and then mapped to the *P. putida* KT2440 reference genome (GenBank: NC_002947.4) using Bowtie2 v.2.3.5.1 (Langmead and Salzberg (2012). Mapped data were converted to BAM files using Samtools v1.11 (Li *et al*., 2009) and reads were visualized with the Integrative Genomics Viewer (IGV) (Robinson *et al*., 2011). Raw dataset is available at the Gene Expression Omnibus (GEO) database (http://www.ncbi.nlm.nih.gov/geo) under accession number GEO: GSE173832.

ACKNOWLEDGMENTS

We wish to thank María G. Velasco, Laura Claret and Álvaro Escobar for their help in some of the constructions used in this work, Guadalupe Martín for technical assistance and all members of the Govantes and Santero laboratories at CABD for providing materials and critical discussion. This work was funded by the Spanish Ministerio de Ciencia, Innovación y Universidades and European Regional Development fund, grants BIO2013-420173-P and PGC2018-097151-B-I00 awarded to FG. M P-S is the recipient of a PhD training grant (FPU) of the Spanish Ministerio de Ciencia, Innovación y Universidades. The authors declare no conflict of interest.

REFERENCES

Albert-Weissenberger, C., Sahr, T., Sismeiro, O., Hacker, J., Heuner, K., and Buchrieser, C. (2010) Control of flagellar gene regulation in *Legionella pneumophila* and its relation to growth phase. J Bacteriol 192: 446–455. https://doi.org/10.1128/JB.00610-09

Altegoer, F., Schuhmacher, J., Pausch, P., and Bange, G. (2014) From molecular evolution to biobricks and synthetic modules: A lesson by the bacterial flagellum. Biotechnol Genet Engin Rev 30: 49–64. https://doi.org/10.1080/02648725.2014.921500

Aranda-Olmedo, I., Tobes, R., Manzanera, M., Ramos, J.L., and Marqués, S. (2002) Species-specific repetitive extragenic palindromic (REP) sequences in *Pseudomonas putida*. Nucleic Acids Res 30: 1826–1833. https://doi.org/10.1093/nar/30.8.1826

Baraquet, C., and Harwood, C. S. (2013) Cyclic diguanosine monophosphate represses bacterial flagella synthesis by interacting with the Walker a motif of the enhancer-binding protein FleQ. Proc Natl Acad Sci USA 110(46), 18478–18483. https://doi.org/10.1073/pnas.1318972110

Baraquet, C., Murakami, K., Parsek, M.R., and Harwood, C.S. (2012) The FleQ protein from *Pseudomonas aeruginosa* functions as both a repressor and an activator to control gene expression from the Pel operon promoter in response to c-di-GMP. Nucleic Acids Res 40: 7207–7218. https://doi.org/10.1093/nar/gks384

Barrios, H., Valderrama, B., and Morett, E. (1999) Compilation and analysis of σ^{54}-dependent promoter sequences. Nucleic Acids Res 27: 4305–4313. https://doi.org/10.1093/nar/27.22.4305

Bhuwan, M., Lees, H.J., Pengs, H.L., and Chang, H.Y. (2012) Histidine-containing phosphotransfer protein-B (HptB) regulates swarming motility through partner-switching system in *Pseudomonas aeruginosa* PAO1 strain. J Biol Chem 287: 1903–1914. https://doi.org/10.1074/jbc.M111.256586

Blagotinsek, V., Schwan, M., Steinchen, W., Mrusek, D., Hook, J. C., Rossmann, F., Freibert, S.A., Kratzat, H., Murat, G., Kressler, D., Beckmann, R., Beeby, M., Thormann, K.M., and Bange, G. (2020) An ATP-dependent partner switch links flagellar C-ring assembly with gene expression. Proc Natl Acad Sci USA 117: 20826–20835. https://doi.org/10.1073/pnas.2006470117

Blanco-Romero, E., Redondo-Nieto, M., Martínez-Granero, F., Garrido-Sanz, D., Ramos-González, M.I., Martín, M., and Rivilla, R. (2018) Genome-wide analysis of the FleQ direct regulon in *Pseudomonas fluorescens* F113 and *Pseudomonas putida* KT2440. Sci Rep 8: 13145. https://doi.org/10.1038/s41598-018-31371-z

Boll, J. M., and Hendrixson, D. R. (2013) A regulatory checkpoint during flagellar biogenesis in *Campylobacter jejuni* initiates signal transduction to activate transcription of flagellar genes. MBio 4: e00432-13. https://doi.org/10.1128/mBio.00432-13

Bouteiller, M., Dupont, C., Bourigault, Y., Latour, X., Barbey, C., Konto-ghiorghi, Y., and Merieau, A. (2021) *Pseudomonas* flagella: Generalities and specificities. Int J Mol Sci 22: 3337. https://doi.org/10.3390/ijms22073337

Bown, J.A., Barne, K.A., Minchin, S.D., and Busby, S.J.W. (1997) Extended -10 promoters. In Mechanisms of transcription. Eckstein, F., and Lilley, D. M. J. (eds) Berlin-Heidelberg: Springer, pp. 41–52. https://doi.org/10.1007/978-3-642-60691-5_4

Burnham, P.M., Kolar, W.P., and Hendrixson, D.R. (2020) A polar flagellar transcriptional program mediated by diverse two-component signal transduction systems and basal flagellar proteins is broadly conserved in polar flagellates. MBio 11: e03107-19 https://doi.org/10.1128/mBio.03107-19

Chevance, F.F.V., and Hughes, K.T. (2008) Coordinating assembly of a bacterial macromolecular machine. Nat Rev Microbiol 6: 455–465. https://doi.org/10.1038/nrmicro1887

Choi, K.H., Gaynor, J.B., White, K.G., Lopez, C., Bosio, C.M., Karkhoff-Schweizer, R.A.R., and Schweizer, H. P. (2005) A Tn7-based broad-range bacterial cloning and expression system. Nat Meth 2: 443–448. https://doi.org/10.1038/nmeth765

Choi, K.H., Kumar, A., and Schweizer, H. P. (2006) A 10-min method for preparation of highly electrocompetent *Pseudomonas aeruginosa* cells: Application for DNA fragment transfer between chromosomes and plasmid transformation. J Microbiol Methods 64: 391–397. https://doi.org/10.1016/j.mimet.2005.06.001

Conway, T., Creecy, J.P., Maddox, S.M., Grissom, J.E., Conkle, T.L., Shadid, T.M., *et al*. (2014) Unprecedented high-resolution view of bacterial operon architecture revealed by RNA sequencing. MBio 5: e01442-14. https://doi.org/10.1128/mBio.01442-14

Corral-Lugo, A., De la Torre, J., Matilla, M.A., Fernández, M., Morel, B., Espinosa-Urgel, M., and Krell, T.

(2016) Assessment of the contribution of chemoreceptor-based signalling to biofilm formation. Environ Microbiol 18: 3355–3372. https://doi.org/10.1111/1462-2920.13170

Correa, N.E., Barker, J.R., and Klose, K.E. (2004) The *Vibrio cholerae* FlgM homologue is an anti-σ^{28} factor that is secreted through the sheathed polar flagellum. J Bacteriol 186: 4613–4619. https://doi.org/10.1128/JB.186.14.4613-4619.2004

Dasgupta, N., Arora, S.K., and Ramphal, R. (2000) *fleN*, a gene that regulates flagellar number in *Pseudomonas aeruginosa*. J Bacteriol 182:, 357–364. https://doi.org/10.1128/JB.182.2.357-364.2000

Dasgupta, N., Ferrell, E.P., Kanack, K.J., West, S.E. H., and Ramphal, R. (2002) *fleQ*, the gene encoding the major flagellar regulator of *Pseudomonas aeruginosa*, is σ^{70} dependent and is downregulated by Vfr, a homolog of *Escherichia coli* cyclic AMP receptor protein. J Bacteriol 184: 5240–5250. https://doi.org/10.1128/JB.184.19.5240-5250.2002

Dasgupta, N., and Ramphal, R. (2001) Interaction of the antiactivator FleN with the transcriptional activator FleQ regulates flagellar number in *Pseudomonas aeruginosa*. J Bacteriol 183: 6636–6644. https://doi.org/10.1128/JB.183.22.6636-6644.2001

Dasgupta, N., Wolfgang, M.C., Goodman, A.L., Arora, S.K., Jyot, J., Lory, S., and Ramphal, R. (2003) A four-tiered transcriptional regulatory circuit controls flagellar biogenesis in *Pseudomonas aeruginosa*. Mol Microbiol 50: 809–824. https://doi.org/10.1046/j.1365-2958.2003.03740.x

Echazarreta, M.A., and Klose, K.E. (2019) *Vibrio* flagellar synthesis. Front Cell Infect Microbiol 9: 131. https://doi.org/10.3389/fcimb.2019.00131

Edgar, R.C. (2004) MUSCLE: A multiple sequence alignment method with reduced time and space complexity. BMC Bioinformatics 5: 13. https://doi.org/10.1186/1471-2105-5-113

Espinosa-Urgel, M., Salido, A., and Ramos, J.L. (2000) Genetic analysis of functions involved in adhesion of *Pseudomonas putida* to seeds. J Bacteriol 182: 2363–2369. https://doi.org/10.1128/JB.182.9.2363-2369.2000

Evans, L.D.B., Hughes, C., and Fraser, G.M. (2014) Building a flagellum outside the bacterial cell. Trends Microbiol 22: 566-572. https://doi.org/10.1016/j.tim.2014.05.009

Frisk, A., Jyot, J., Arora, S.K., and Ramphal, R. (2002) Identification and functional characterization of *flgM*, a gene encoding the anti-sigma 28 factor in *Pseudomonas aeruginosa*. J Bacteriol 184: 1514–1521. https://doi.org/10.1128/JB.184.6.1514-1521.2002

Gao, T., Shi, M., and Gao, H. (2018) Partially reciprocal replacement of FlrA and FlrC in regulation of *Shewanella oneidensis* flagellar biosynthesis. J Bacteriol 200: e00796-17 https://doi.org/10.1128/JB.00796-17

García-Fontana, C., Reyes-Darias, J.A., Muñoz-Martínez, F., Alfonso, C., Morel, B., Ramos, J.L., and Krell, T. (2013) High specificity in CheR methyltransferase function: CheR2 of *Pseudomonas putida* is essential for chemotaxis, whereas CheR1 is involved in biofilm formation. J Biol Chem 288: 18987–18999. https://doi.org/10.1074/jbc.M113.472605

García-González, V., Govantes, F., Porrúa, O., and Santero, E. (2005) Regulation of the *Pseudomonas* sp. strain ADP cyanuric acid degradation operon. L Bacteriol 187: 155-167. https://doi.org/10.1128/JB.187.1.155-167.2005.

Green, J.C.D., Kahramanoglou, C., Rahman, A., Pender, A.M.C., Charbonnel, N., and Fraser, G.M. (2009) Recruitment of the earliest component of the bacterial flagellum to the old cell division pole by a membrane-associated Signal Recognition Particle family GTP-binding protein. J Mol Biol 391: 679–690. https://doi.org/10.1016/j.jmb.2009.05.075

Gross, R., Hauer, B., Otto, K., and Schmid, A. (2007) Microbial biofilms: New catalysts for maximizing productivity of long-term biotransformations. Biotechnol Bioeng 98: 1123–1134. https://doi.org/10.1002/bit.21547

Harwood, C.S., Fosnaugh,K., and Dispensa, M. (1989) Flagellation of *Pseudomonas putida* and analysis of its motile behavior. J Bacteriol 171: 4063–4066. https://doi.org/10.1128/jb.171.7.4063-4066.1989

Hickman, J.W., and Harwood, C.S. (2008) Identification of FleQ from *Pseudomonas aeruginosa* as a c-di-GMP-responsive transcription factor. Mol Microbiol 69: 376–389. https://doi.org/10.1111/j.1365-2958.2008.06281.x

Hoang, T.T., Karkhoff-Schweizer, R.R., Kutchma, A.J., and Schweizer, H.P. (1998) A broad-host-range Flp-FRT recombination system for site-specific excision of chromosomally-located DNA sequences: Application for isolation of unmarked *Pseudomonas aeruginosa* mutants. Gene 212: 77–86. https://doi.org/10.1016/S0378-1119(98)00130-9

Inoue, H., Nojima, H., and Okayama, H. (1990) High efficiency transformation of *Escherichia coli* with plasmids.

Gene 96: 23–28. https://doi.org/10.1016/0378-1119(90)90336-P

Jacob, F., and Monod, J. (1961) Genetic regulatory mechanisms in the synthesis of proteins. J Mol Biol 3: 318–356. https://doi.org/10.1016/S0022-2836(61)80072-7

Jiménez-Fernández, A., López-Sánchez, A., Jiménez-Díaz, L., Navarrete, B., Calero, P., Platero, A.I., and Govantes, F. (2016) Complex Interplay between FleQ, cyclic diguanylate and multiple σ factors coordinately regulates flagellar motility and biofilm development in *Pseudomonas putida*. PLoS One 11: 1–26. https://doi.org/10.1371/journal.pone.0163142

Karlinsey, J.E., Tanaka, S., Bettenworth, V., Yamaguchi, S., Boos, W., Aizawa, S. I., and Hughes, K.T. (2000) Completion of the hook-basal body complex of the *Salmonella typhimurium* flagellum is coupled to FlgM secretion and fliC transcription. Mol Microbiol 37: 1220-1231. https://doi.org/10.1046/j.1365-2958.2000.02081.x

Kearns, D.B. (2010) A field guide to bacterial swarming motility. Nat Rev Microbiol 8: 634–644. https://doi.org/10.1038/nrmicro2405

Khan, F., Tabassum, N., Anand, R., and Kim, Y.M. (2020) Motility of *Vibrio* spp.: regulation and controlling strategies. Appl Microbiol Biotechnol 104: 8187–8208. https://doi.org/10.1007/s00253-020-10794-7

Kim, J.S., Kim, Y.H., Anderson, A.J., and Kim, Y.C. (2014) The sensor kinase GacS negatively regulates flagellar formation and motility in a biocontrol bacterium, *Pseudomonas chlororaphis* O6. Plant Pathol J 30: 215–219. https://doi.org/10.5423/PPJ.NT.11.2013.0109

Kim, Y.K., and McCarter, L.L. (2000) Analysis of the polar flagellar gene system of *Vibrio parahaemolyticus*. J Bacteriol 188: 852-862. https://doi.org/10.1128/JB.182.13.3693-3704.2000

Langmead, B., and Salzberg, S.L. (2012) Fast gapped-read alignment with Bowtie 2. Nat Meth 9: 357–359. https://doi.org/10.1038/nmeth.1923

Li, H., Handsaker, B., Wysoker, A., Fennell, T., Ruan, J., Homer, N. *et al*. (2009) The Sequence Alignment/Map format and SAMtools. Bioinformatics 25: 2078–2079. https://doi.org/10.1093/bioinformatics/btp352

Li, X.Z., Hauer, B., and Rosche, B. (2007) Single-species microbial biofilm screening for industrial applications. Appl Microbiol Biotechnol 76: 1255–1262. https://doi.org/10.1007/s00253-007-1108-4

Llamas, M.A., Ramos, J.L., and Rodriguez-Herva, J.J. (2000) Mutations in each of the *tol* genes of *Pseudomonas putida* reveal that they are critical for maintenance of outer membrane stability. J Bacteriol 182: 4764–4772. https://doi.org/10.1128/JB.182.17.4764-4772.2000

Ma, Y., Liu, Y., Bi, Y., Han, X., Jin, Y., Xu, H., and Qiao, M. (2021) OsaR (PA0056) functions as a repressor of the gene *fleQ* encoding an important motility regulator in *Pseudomonas aeruginosa* . J Bacteriol, in press. https://doi.org/10.1128/jb.00145-21

Markel, E., Dalenberg, H., Monteil, C.L., Vinatzer, B.A., and Swingle, B. (2018) An AlgU-regulated antisense transcript encoded within the *Pseudomonas syringae fleQ* gene has a positive effect on motility. J Bacteriol 200:e00576-17. https://doi.org/10.1128/JB.00576-17

Martínez-García, E., and de Lorenzo, V. (2011) Engineering multiple genomic deletions in Gram-negative bacteria: Analysis of the multi-resistant antibiotic profile of *Pseudomonas putida* KT2440. Environ Microbiol 13: 2702–2716. https://doi.org/10.1111/j.1462-2920.2011.02538.x

Martínez-García, E., and De Lorenzo, V. (2012) Transposon-based and plasmid-based genetic tools for editing genomes of Gram-negative bacteria. Methods Mol Biol 813: 267–283. https://doi.org/10.1007/978-1-61779-412-4_16

Martínez-García, E., Nikel, P.I., Chavarría, M., and de Lorenzo, V. (2014) The metabolic cost of flagellar motion in *Pseudomonas putida* KT2440. Environ Microbiol 16: 291–303. https://doi.org/10.1111/1462-2920.12309

Martínez-Granero, F., Navazo, A., Barahona, E., Redondo-Nieto, M., Rivilla, R., and Martín, M. (2012) The Gac-Rsm and SadB signal transduction pathways converge on AlgU to downregulate motility in *Pseudomonas fluorescens*. PLoS One 7: e31765 https://doi.org/10.1371/journal.pone.0031765

Martins Dos Santos, V.A.P., Heim, S., Moore, E.R.B., Strätz, M., and Timmis, K.N. (2004) Insights into the genomic basis of niche specificity of *Pseudomonas putida* KT2440. Environ Microbiol 6: 1264–1286. https://doi.org/10.1111/j.1462-2920.2004.00734.x

McCarter, L.L. (2001) Polar Flagellar Motility of the Vibrionaceae . Microbiol Mol Biol Rev 65: 445–462. https://doi.org/10.1128/mmbr.65.3.445-462.2001

McDougald, D., Rice, S.A., Barraud, N., Steinberg, P.D., and Kjelleberg, S. (2012) Should we stay or should we go: Mechanisms and ecological consequences for biofilm dispersal. Nat Rev Microbiol 10: 39–50.

https://doi.org/10.1038/nrmicro2695

Miller, J.H. (1993) A short course in bacterial genetics - A laboratory manual and handbook for *Escherichia coli* and related bacteria. Cold Spring Harbor, New York, USA: Cold Spring Harbor Laboratory Press.

Moisi, M., Jenul, C., Butler, S.M., New, A., Tutz, S., Reidl, J. *et al*. (2009) A novel regulatory protein involved in motility of *Vibrio cholerae*. J Bacteriol 191: 7027–7038. https://doi.org/10.1128/JB.00948-09

Navarrete, B., Leal-Morales, A., Serrano-Ron, L., Sarrió, M., Jiménez-Fernández, A., Jiménez-Díaz, L. *et al*. (2019) Transcriptional organization, regulation and functional analysis of *flhF* and *fleN* in *Pseudomonas putida*. PLoS One 14: e0214166. https://doi.org/10.1371/journal.pone.0214166

Pallen, M.J., Penn, C.W., and Chaudhuri, R.R. (2005) Bacterial flagellar diversity in the post-genomic era. Trends Microbiol 13: 143–149. https://doi.org/10.1016/j.tim.2005.02.008

Parkinson, J.S. (1976) *cheA*, *cheB*, and *cheC* genes of *Escherichia coli* and their role in chemotaxis. J Bacteriol 126: 758–770. https://doi.org/10.1128/jb.126.2.758-770.1976

Petersen, B.D., Liu, M.S., Podicheti, R., Yang, A.Y.-P., Simpson, C.A., Hemmerich, C. *et al*. (2021) The polar flagellar transcriptional regulatory network in *Vibrio campbellii* deviates from canonical *Vibrio* species . J Bacteriol, in press. https://doi.org/10.1128/jb.00276-21

Poggio, S., Osorio, A., Dreyfus, G., and Camarena, L. (2005) The flagellar hierarchy of *Rhodobacter sphaeroides* is controlled by the concerted action of two enhancer-binding proteins. Mol Microbiol 58: 969–983. https://doi.org/10.1111/j.1365-2958.2005.04900.x

Prouty, M.G., Correa, N.E., and Klose, K.E. (2001) The novel σ^{54}- and σ^{28}-dependent flagellar gene transcription hierarchy of *Vibrio cholerae*. Mol Microbiol 39: 1595–1609. https://doi.org/10.1046/j.1365-2958.2001.02348.x

Ringgaard, S., Yang, W., Alvarado, A., Schirner, K., and Briegel, A. (2018) Chemotaxis arrays in *Vibrio* species and their intracellular positioning by the ParC/ParP system. J Bacteriol 200: e00793. https://doi.org/10.1128/JB.00793-17

Robinson, J.T., Thorvaldsdóttir, H., Winckler, W., Guttman, M., Lander, E.S., Getz, G., and Mesirov, J.P. (2011) Integrative genomics viewer. Nat Biotechnol 29: 24–26. https://doi.org/10.1038/nbt.1754

Rodríguez-Herva, J.J., Duque, E., Molina-Henares, M A., Navarro-Avilés, G., van Dillewijn, P., de la Torre, J. *et al*. (2010) Physiological and transcriptomic characterization of a *fliA* mutant of *Pseudomonas putida* KT2440. Environ Microbiol Rep 2: 373–380. https://doi.org/10.1111/j.1758-2229.2009.00084.x

Sambrook, J.E., and Russell, D.W. (2000) Molecular Cloning, a Laboratory Manual. Cold Spring Harbor, New York, USA: Cold Spring Harbor Laboratory Press.

Schuhmacher, J.S., Rossmann, F., Dempwolff, F., Knauer, C., Altegoer, F., Steinchen, W. *et al*. (2015) MinD-like ATPase FlhG effects location and number of bacterial flagella during C-ring assembly. Proc Natl Acad Sci USA 112: 3092–3097. https://doi.org/10.1073/pnas.1419388112

Schuhmacher, J.S., Thormann, K.M., and Bange, G. (2015) How bacteria maintain location and number of flagella?. FEMS MIcrobiol Rev 39: 812–822. https://doi.org/10.1093/femsre/fuv034

Shi, M., Gao, T., Ju, L., Yao, Y., and Gao, H. (2014) Effects of FlrBC on flagellar biosynthesis of *Shewanella oneidensis*. Mol Microbiol 93: 1269–1283. https://doi.org/10.1111/mmi.12731

Smith, T.G., and Hoover, T.R. (2009) Deciphering bacterial flagellar gene regulatory networks in the genomic era. Adv Appl Microbiol 67: 257-295. https://doi.org/10.1016/S0065-2164(08)01008-3

Smith, T. G., Pereira, L., and Hoover, T. R. (2009) Helicobacter pylori FlhB processing-deficient variants affect flagellar assembly but not flagellar gene expression. Microbiology 155(4), 1170–1180. https://doi.org/10.1099/mic.0.022806-0

Sourjik, V., and Wingreen, N.S. (2012) Responding to chemical gradients: Bacterial chemotaxis. Curr Opin Cell Biol 24: 262–268. https://doi.org/10.1016/j.ceb.2011.11.008

Tart, A.H., Blanks, M.J., and Wozniak, D.J. (2006) The AlgT-dependent transcriptional regulator AmrZ (AlgZ) inhibits flagellum biosynthesis in mucoid, nonmotile *Pseudomonas aeruginosa* cystic fibrosis isolates. J Bacteriol 188: 6483–6489. https://doi.org/10.1128/JB.00636-06

Tart, A.H., Wolfgang, M.C., and Wozniak, D.J. (2005) The alternative sigma factor AlgT represses *Pseudomonas aeruginosa* flagellum biosynthesis by inhibiting expression of fleQ. J Bacteriol 187: 7955–7962. https://doi.org/10.1128/JB.187.23.7955-7962.2005

Terashima, H., Kojima, S., and Homma, M. (2008) Flagellar motility in bacteria. Structure and function of flagellar motor. Int Rev Cell Mol Biol 270: 39-85. https://doi.org/10.1016/S1937-6448(08)01402-0

Toutain, C.M., Zegans, M.E., and O'Toole, G.A. (2005) Evidence for two flagellar stators and their role in the motility of *Pseudomonas aeruginosa*. J Bacteriol 187: 771–777. https://doi.org/10.1128/JB.187.2.771-777.2005

Tsang, J., and Hoover, T.R. (2015) Basal body structures differentially affect transcription of RpoN and FliA-dependent flagellar genes in *Helicobacter pylori*. J Bacteriol 197: 1921–1930. https://doi.org/10.1128/JB.02533-14

Valentini, M., Laventie, B.J., Moscoso, J., Jenal, U., and Filloux, A. (2016) The diguanylate cyclase HsbD intersects with the HptB regulatory cascade to control *Pseudomonas aeruginosa* biofilm and motility. PLoS Genet 12: e1006354 https://doi.org/10.1371/journal.pgen.1006354

Vera, J.M., Ghosh, I.N., Zhang, Y., Hebert, A.S., Coon, J.J., and Landick, R. (2020) Genome-scale transcription-translation mapping reveals features of *Zymomonas mobilis* transcription units and promoters. mSystems 5: e00250-20. https://doi.org/10.1128/msystems.00250-20

Wand, M.E., Sockett, R.E., Evans, K.J., Doherty, N., Sharp, P.M., Hardie, K.R., and Winzer, K. (2006) *Helicobacter pylori* FlhB function: The FlhB C-terminal homologue HP1575 acts as a "spare part" to permit flagellar export when the HP0770 FlhBCC domain is deleted. J Bacteriol 188: 7531–7541. https://doi.org/10.1128/JB.00263-06

Wang, Y., Li, Y., Wang, J., and Wang, X. (2018) FleQ regulates both the type VI secretion system and flagella in *Pseudomonas putida*. Biotechnol Appl Chem 65: 419–427. https://doi.org/10.1002/bab.1611

Warrier, I., Ram-Mohan, N., Zhu, Z., Hazery, A., Echlin, H., Rosch, J. *et al*. (2018) The Transcriptional landscape of *Streptococcus pneumoniae* TIGR4 reveals a complex operon architecture and abundant riboregulation critical for growth and virulence. PLoS PAthog 14: e1007461. https://doi.org/10.1371/journal.ppat.1007461

Wilhelms, M., Molero, R., Shaw, J.G., Tomás, J. M., and Merino, S. (2011) Transcriptional hierarchy of *Aeromonas hydrophila* polar-flagellum genes. J Bacteriol 193: 5179–5190. https://doi.org/10.1128/JB.05355-11

Winsor, G.L., Griffiths, E.J., Lo, R., Dhillon, B.K., Shay, J.A., and Brinkman, F.S.L. (2016) Enhanced annotations and features for comparing thousands of *Pseudomonas* genomes in the *Pseudomonas* genome database. Nucleic Acids Res 44: D646–D653. https://doi.org/10.1093/nar/gkv1227

Wirebrand, L., Österberg, S., López-Sánchez, A., Govantes, F., and Shingler, V. (2018) PP4397/FlgZ provides the link between PP2258 c-di-GMP signalling and altered motility in *Pseudomonas putida*. Sci Rep 8: 12205. https://doi.org/10.1038/s41598-018-29785-w

Wu, L., Wang, J., Tang, P., Chen, H., and Gao, H. (2011) Genetic and molecular characterization of flagellar assembly in *Shewanella oneidensis*. PLoS One 6: e21479. https://doi.org/10.1371/journal.pone.0021479

Yan, B., Boitano, M., Clark, T.A., and Ettwiller, L. (2018) SMRT-Cappable-seq reveals complex operon variants in bacteria. Nat Commun 9: 3676. https://doi.org/10.1038/s41467-018-05997-6

Zhou, T., Huang, J., Liu, Z., Xu, Z., and Zhang, L. (2021) Molecular mechanisms underlying the regulation of biofilm formation and swimming motility by FleS/FleR in *Pseudomonas aeruginosa*. Front Microbiol 12: 707711. https://doi.org/10.3389/fmicb.2021.707711

FIGURES

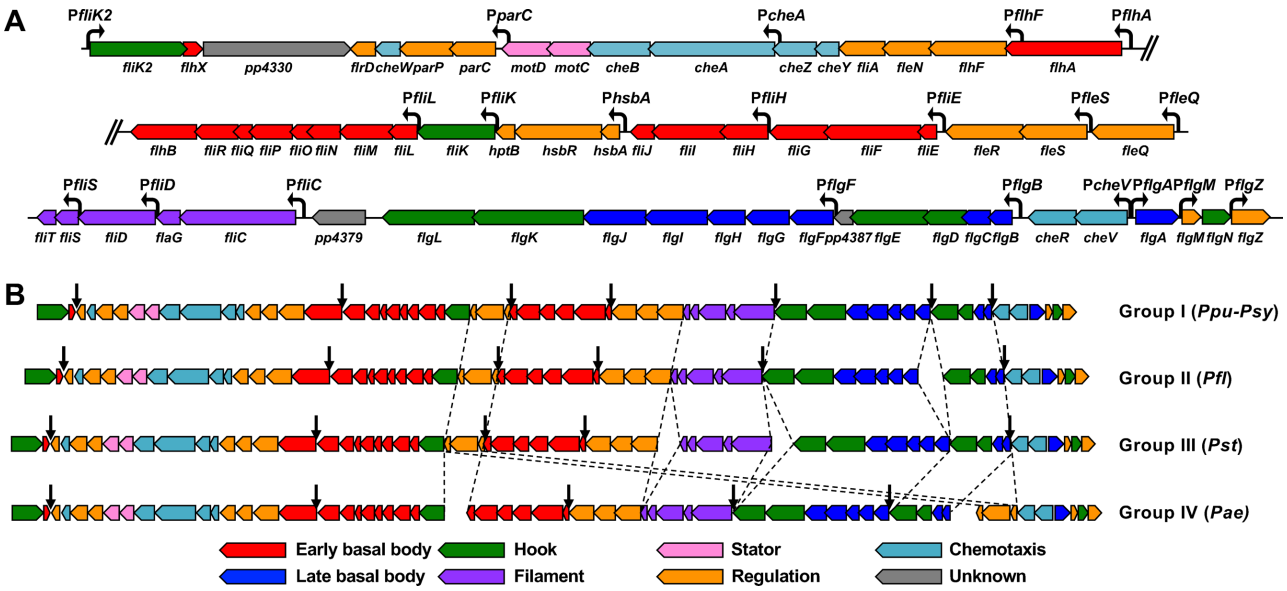

Figure 1. The *Pseudomonas* flagellar cluster. Synteny relationships between the 59 flagella-related genes in the *Pseudomonas* flagellar cluster. Genes are color-coded to denote their putative function as indicated. **A.** Cartoon of the *P. putida* KT2440 flagellar cluster, including designations of all 59 flagella-related genes and the 20 promoters identified in this work. The 7-gene insertion (PP_4345 to PP_4351) upstream from *flhA* is omitted (indicated by two oblique lines). **B.** Simplified cartoons of the *Pseudomonas* Group I, II, III and IV flagellar clusters. Dashed lines indicate points of synteny disruption between groups. Black arrows indicate preferential locations for insertion of small groups of additional genes.

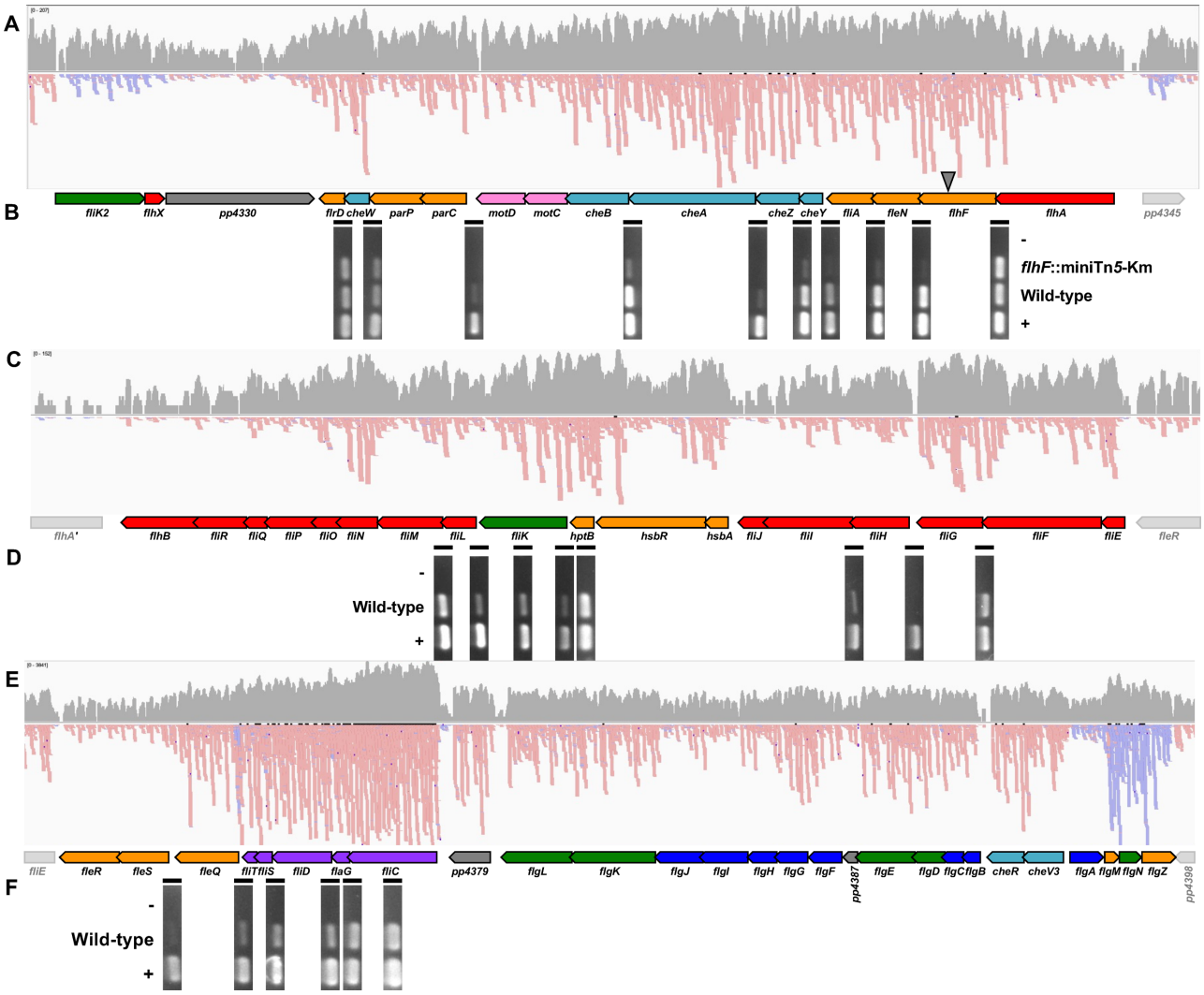

Figure 2. RNA-seq and RT-PCR analysis of the transcriptional organization of the *P. putida* flagellar cluster. A., **C.** and **E.** Output of the RNA-seq analysis of the KT2440 flagellar cluster, split in three regions. Coverage is represented in grey on a logarithmic scale. Top strand and bottom strand reads are shown in blue and pink, respectively. **B.**, **D.** and **F.** Agarose gel electrophoresis showing the RT-PCR results for selected regions of the *flhAF-fleN-flhF-fliA-cheYZAB-motCD-parCP-cheW-flrD* (**B**), *hsbAR-hptB-fliKLMNOPQR-flhB*, *fliEFG and fliHIJ* (**C**) and *fliC-flaG-fliDST-fleQSR* (**F**) operons. Plus (+) and minus (-) signs denote PCR reactions performed with genomic DNA and RNA, respectively, as templates. A cartoon of the flagellar genes is aligned with the RNA-seq reads and RT-PCR results. Genes are color-coded as in **Fig. 1.** An inverted triangle denotes the location of the *flhF*::miniTn*5*-Km insertion. The RNA-seq images represent data from a single representative replicate. Each RT-PCR image was cropped from a single picture and represents consecutive lanes of a representative agarose gel.

```
A
                    σ54 consensus
                    TGGCACG-N4- TTGCw
PparC   TGCGCCGGGCTGGCACACAAAGTGCACCGGCAATAC
PflhF   GAGCCAAGGTTGGAACAGATTTTGCTGAATAGTCTG
PflhA   CTGCCAAAGTTGGAAAGCTTCTTGCAAAGCCACGCC
PfliL   CTGCAAAATCTGGCATAACACTTGCTCAAGCCAAGC
PfliK   ATACGCGAGTTGGCGCGAGTCTTGCCTGTCTCTGCC
PfliE   TTGCGAAGGCTGGCACCTTTGTTGCTTTAGGTAGGT
PfleS   CCCCCATCTCCGGCACGGCTATTGCTACACCGCTGG
PfliD   TGTGTAATGTTGGCATGAGTCTTGACTCGGATTGTG
PflgF   GTTTCAGACTTGGTTCAATTATTGCTTGGAACCTGC
PflgB   TTCCAGTGGTTGGCACAGCCCTTGCTATGCCTTGCT
PflgA   GGTAGCGAGTCGGCACGGGCTTTGCTTTTTTGAGTG
PflgZ   CAGAACATAGTGGCAAAATGCCGTTACTTGCGTGTG

B
                    FliA consensus
                    TcAAgNw     -N12-13-    gcCGAtaNc
PfliK2  CCCTTGTGTCTCAAGTCGCCCCG-CGCGCTGCCGTTATACTGGCAACCA
PcheA   CGACTCGGGGTGAAGGTCCGCAG-ATTCATGCCGATAAGCGTGAAGACG
PfliS   ATGGTCGTATTCAAGATCTTTGG-GGCTAAGCCGATCACTTAGGTATGT
PfliC   GAAAAAACCCTCAAGCAACCCGC-GCACCCGACGATAACCATTACGAAG
PcheV   AACGGTGAATTCAAGAAACCCTTGGGTGACACCGATAAGCTGTTCAGGC
PflgM   CATTTGTGCCTAAAGTTTATATC-GGGTTGGCCGAAAACAAGGCAAGCG
PmotA   ATTGAGTGGCTATAGTCTGGCGC AGTTCTGCCGATAAGTAGAAGAAGA

C
                    σ70 consensus (extended -10)
                    TTGACA      -N14-15-    TGNTATAaT
PhsbA   CTGCATCCGCTTGCCTCCCCCACCATCGCCTGCTAAACCTTAAAGCAGT
PfleQ   CGCCATAAATTTGACTGCCTTTAAGTTTTTGACTTTACTAGTGGCTGTT
```

Figure 3. The *P. putida* KT2440 flagellar promoter set. Sequences of the twenty-one putative *P. putida* KT2440 flagellar promoters identified in this work, along with the consensus sequences for the corresponding σ factors: σ^{54} (**A**), FliA (**B**) and σ^{70} (**C**). The promoter motifs are indicated in red, and the coding sequences of the upstream genes are indicated in blue.

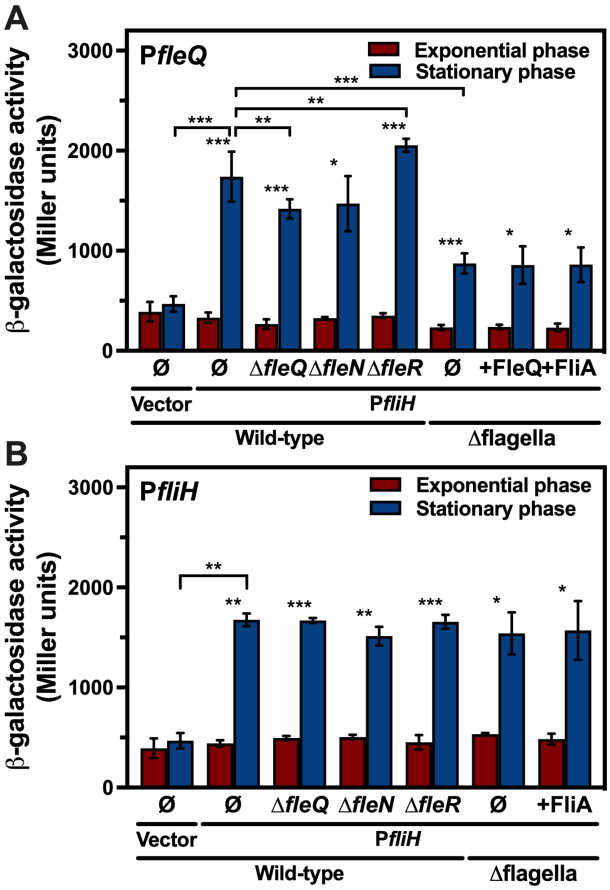

Figure 4. Expression of the P*fleQ* promoter in *P. putida*. β-galactosidase assays of the P*fleQ* (**B**) and P*fliH* (**B**) promoter fusions in the wild-type strain KT2442 and its Δ*fleQ*, Δ*fleN*, Δ*fleR*, Δflagella and Δflagella ectopically expressing FleQ or FliA derivatives. **Ø** denotes no further modification of the genetic background indicated below. Bars represent the averages and standard deviations of at least three independent assays. Stars designate p-values for the Student's t-test for unpaired samples not assuming equal variance. *: p<0.05; **: p<0.01; *:p<0.001.

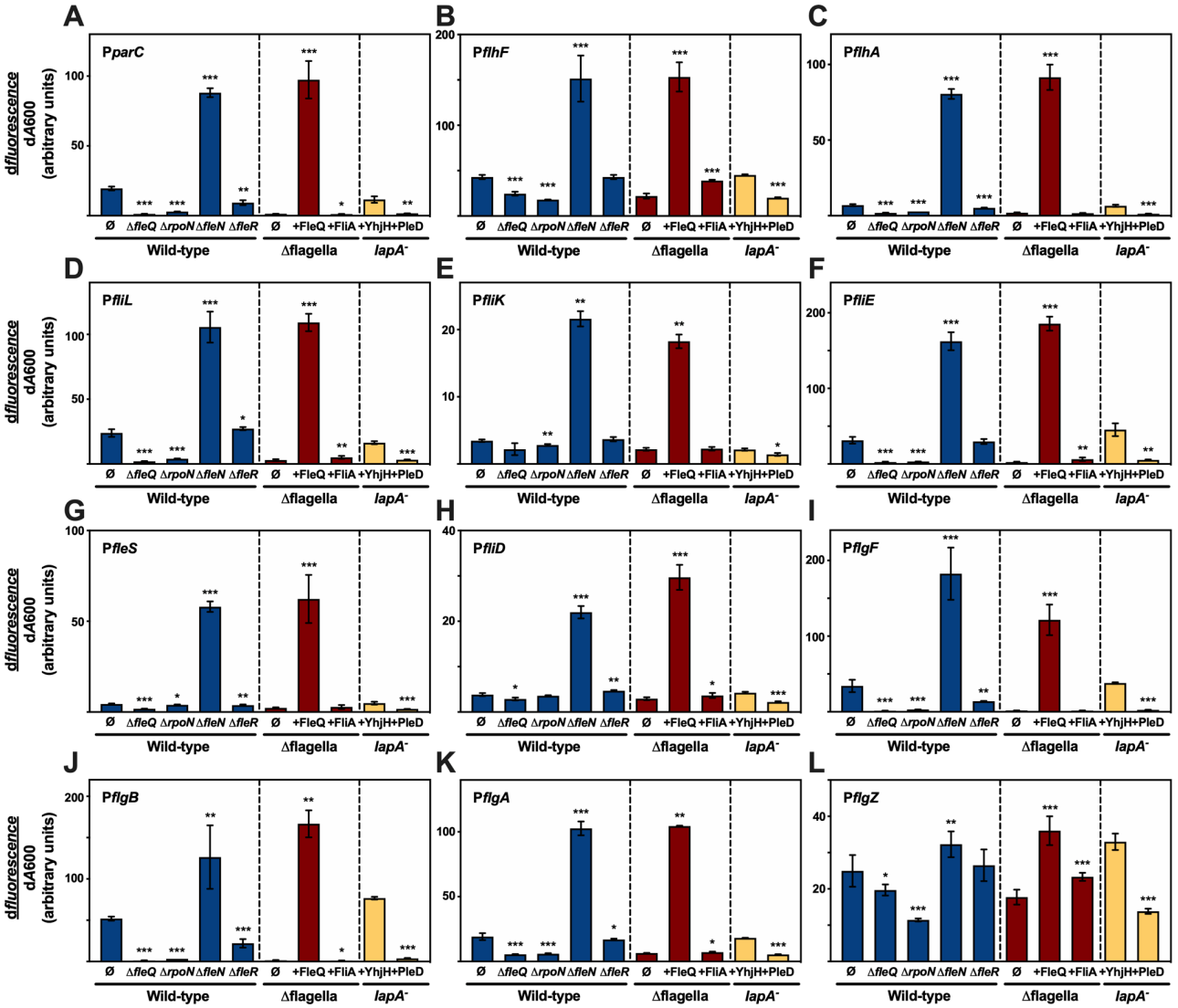

Figure 5. Expression the Class II flagellar promoters in *P. putida*. Differential rates of GFP fluorescence accumulation of the P*parC* (**A**), P*flhF* (**B**), P*flhA* (**C**), P*fliL* (**D**), P*fliK*(**E**), P*fliE* (**F**), P*fleS* (**G**), P*fliD* (**H**), P*flgF* (**I**), P*flgB* (**J**), P*flgA* (**K**) and P*flgZ* (**L**) promoters in the wild-type strain KT2442 and its Δ*fleQ*, Δ*rpoN*, Δ*fleN*, Δ*fleR*, Δflagella, Δflagella ectopically expressing FleQ or FliA, and *lapA*$^-$ expressing YhjH or PleD derivatives. **Ø** denotes no further modification of the genetic background indicated below. Bars represent the averages and standard deviations of at least three independent assays. Stars designate p-values for the Student's t-test for unpaired samples not assuming equal variance. *: p<0.05; **: p<0.01; *:p<0.001.

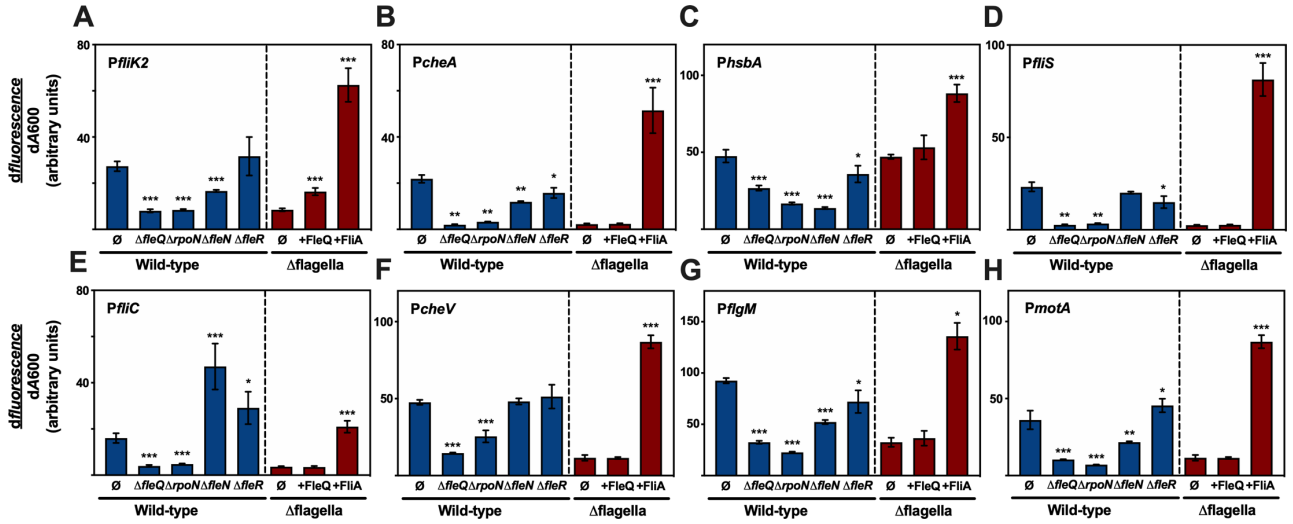

Figure 6. Expression the Class III flagellar promoters in *P. putida*. Differential rates of GFP fluorescence accumulation of the P*fliK2* (**A**), P*cheA* (**B**), P*hsbA* (**C**), P*fliS* (**D**), P*fliC*(**E**), P*cheV* (**F**), P*flgM* (**G**) and P*motA* (**H**) promoters in the wild-type strain KT2442 and its Δ*fleQ*, Δ*rpoN*, Δ*fleN*, Δ*fleR*, Δflagella and Δflagella ectopically expressing FleQ or FliA. **Ø** denotes no further modification of the genetic background indicated below. Bars represent the averages and standard deviations of at least three independent assays. Stars designate p-values for the Student's t-test for unpaired samples not assuming equal variance. *: p<0.05; **: p<0.01; *:p<0.001.

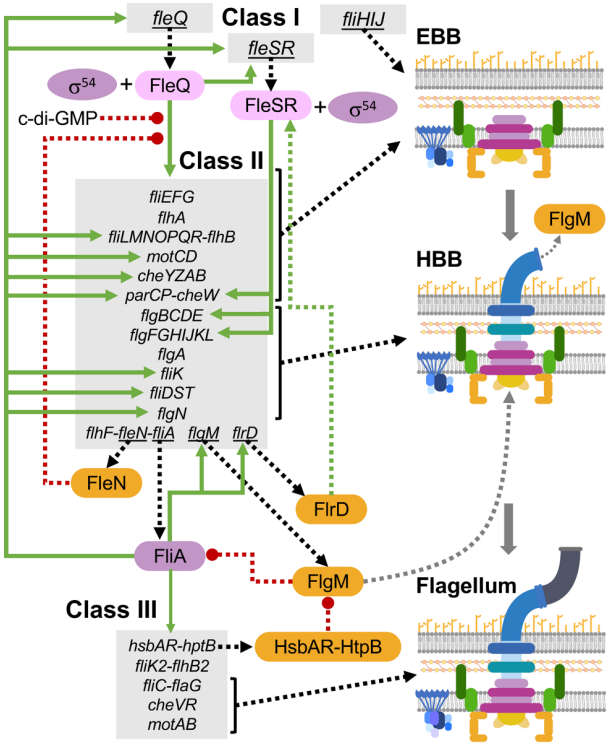

Figure 7. Hypothetical model of the flagellar transcriptional cascade in *P. putida*. Cartoon representing the transcriptional hierarchy, feed-forward and feedback loops of the *P. putida* KT2440 flagellar cascade. Genes are shaded in grey, transcription factors are shaded in pink, σ factors are shaded in purple. and auxiliary regulatory proteins are shaded in orange. Transcription is shown as green arrows and translation is shown as black dashed arrows. Green dashed arrows and red dashed lines with a round end denote positive and regulatory events based on protein-protein interaction, respectively. FlgM secretion by way of the fT3SS is denoted by a dashed grey arrow. Three stages of flagellar assembly are represented: early basal body (EBB), the hook-basal body complex (HBB), and the complete flagellum.